

J-PAS



The Javalambre-Physics of the Accelerating
Universe Astrophysical Survey

Renato Dupke
ON/UM

J-PAS Builder Institutions



Observatório
Nacional

Rio de Janeiro

IAG-USP



COLLABORATION BOARD:

Javier Cenarro (CEFCA)

Renato Dupke (ON)

José (Pepe) Vilchez (IAA)

Laerte Sodre (IAG-USP)



Benitez et al. 2009 –
Simulated with lower (by
>10) resolution
templates and 300A
filters)

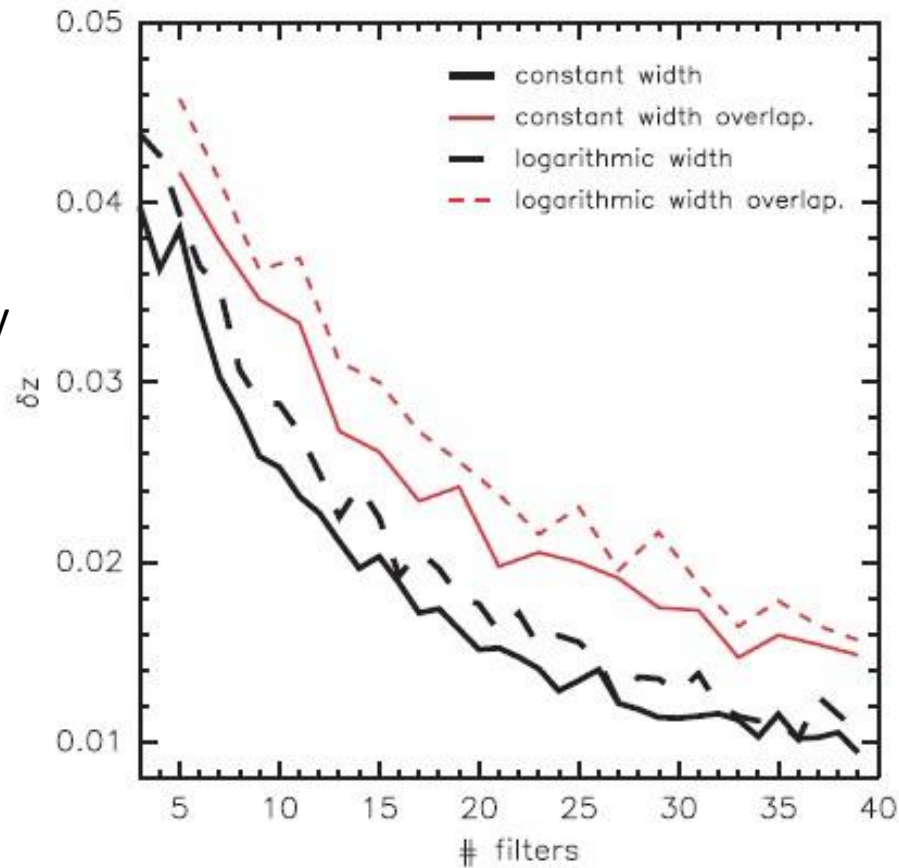
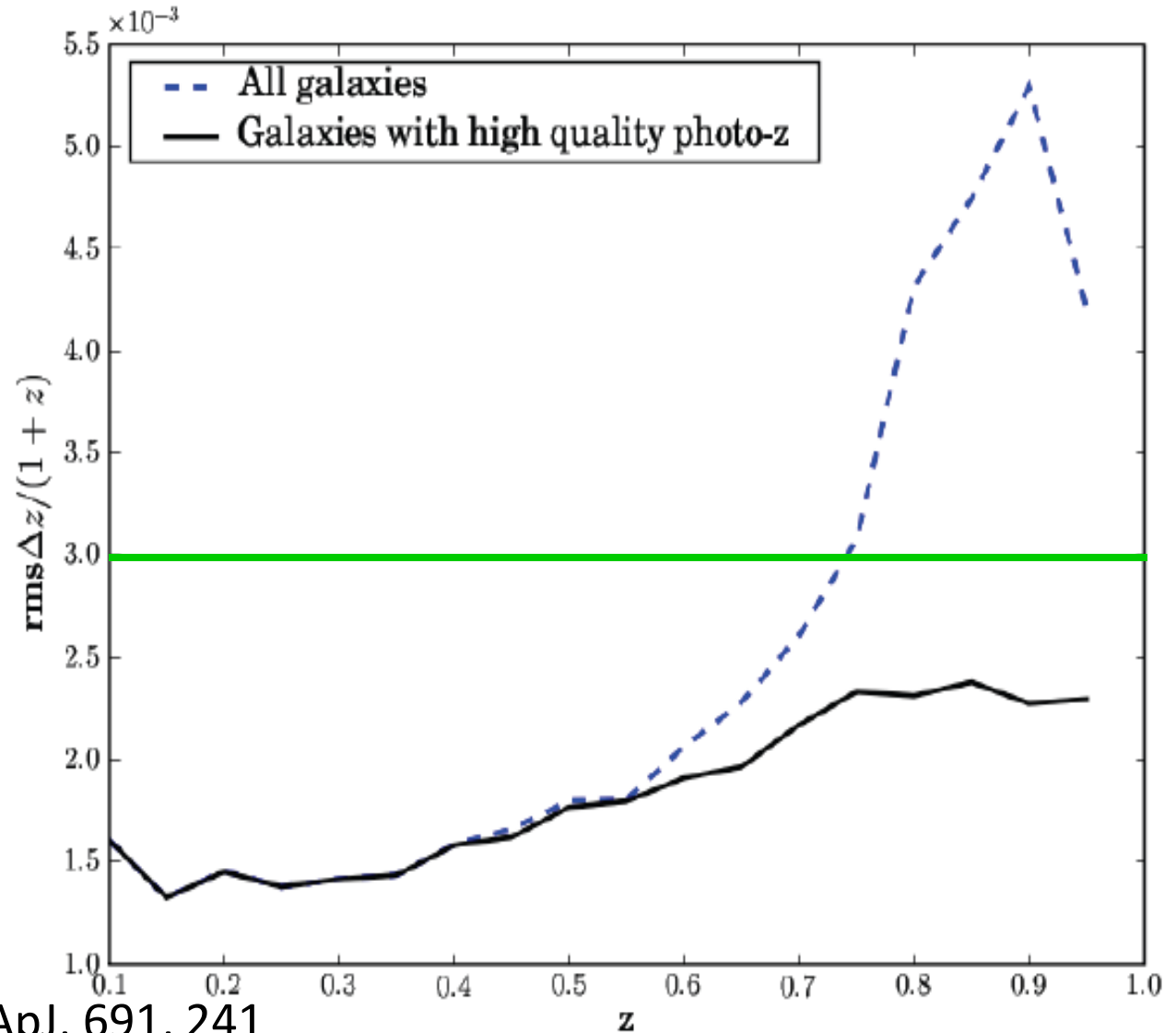


Figure 4. Dependence of the rms of quantity $(z - z_b)/(1 + z)$ for those galaxies with odds > 0.99 as a function of the number of filters for the four types of filter systems considered in the Letter and including near-IR observations (see

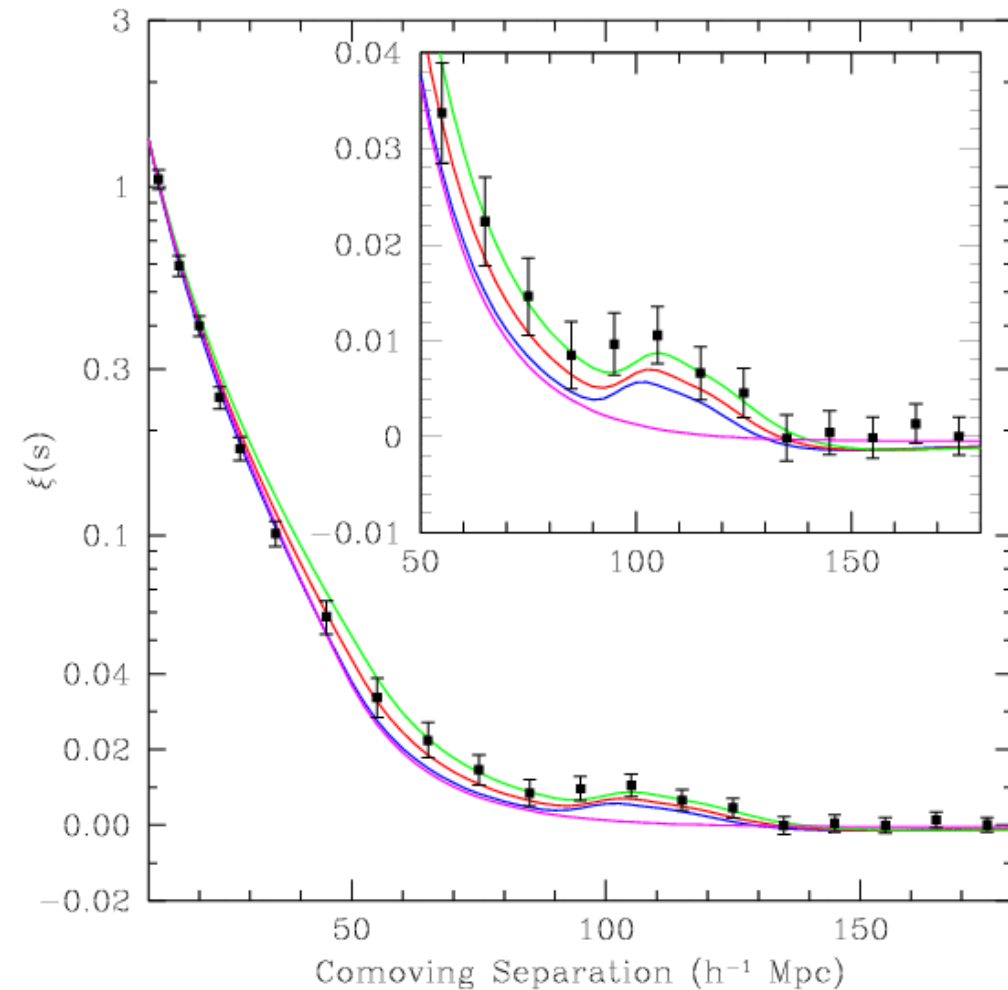
Δz r.m.s as a function of the true z

Bayesian photo- z quality indicator (“BPZ odds”) can select galaxies with high precision photo- z

Measuring the BAO radial scale requires quasi-spectroscopic precision: $0.003(1+z)$.



BAO measured in SDSS data (Eisenstein et al. 2005)



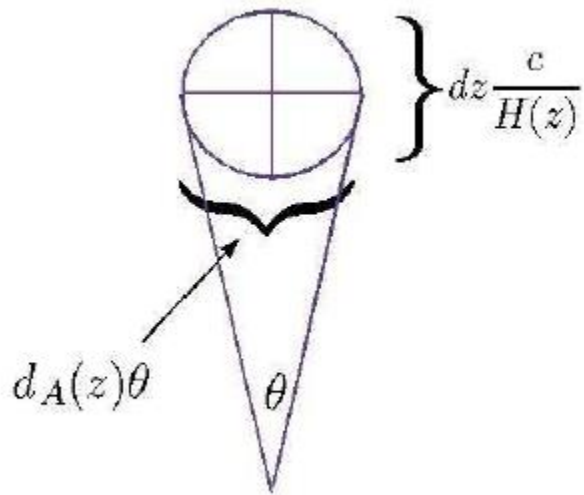
$$\xi(r) = \langle \delta(\vec{r}_1) \delta(\vec{r}_2) \rangle, \delta(\vec{r}) = \frac{\rho(\vec{r}) - \bar{\rho}}{\bar{\rho}}$$

3.5- σ detection of BAO

BUT even better to get radial!

For a flat universe

$$H(z) = h \sqrt{\Omega_m (1+z)^3 + \Omega_X \exp \left[3 \int_0^z \frac{1+w(z)}{1+z} dz \right]}$$



- If we could measure $H(z)$, we would get the dark energy density evolution
- However it is easy to measure **a** (redshift) but not **da/dt**
- We can indirectly measure $H(z)$ through the measurement of distances:

$$D_A(z) = \frac{c}{1+z} \int_0^z \frac{dz}{H(z)}$$

To measure dw/dz we need $d^2H(z)/dz^2$ or $d^3D_A(z)/dz^3$

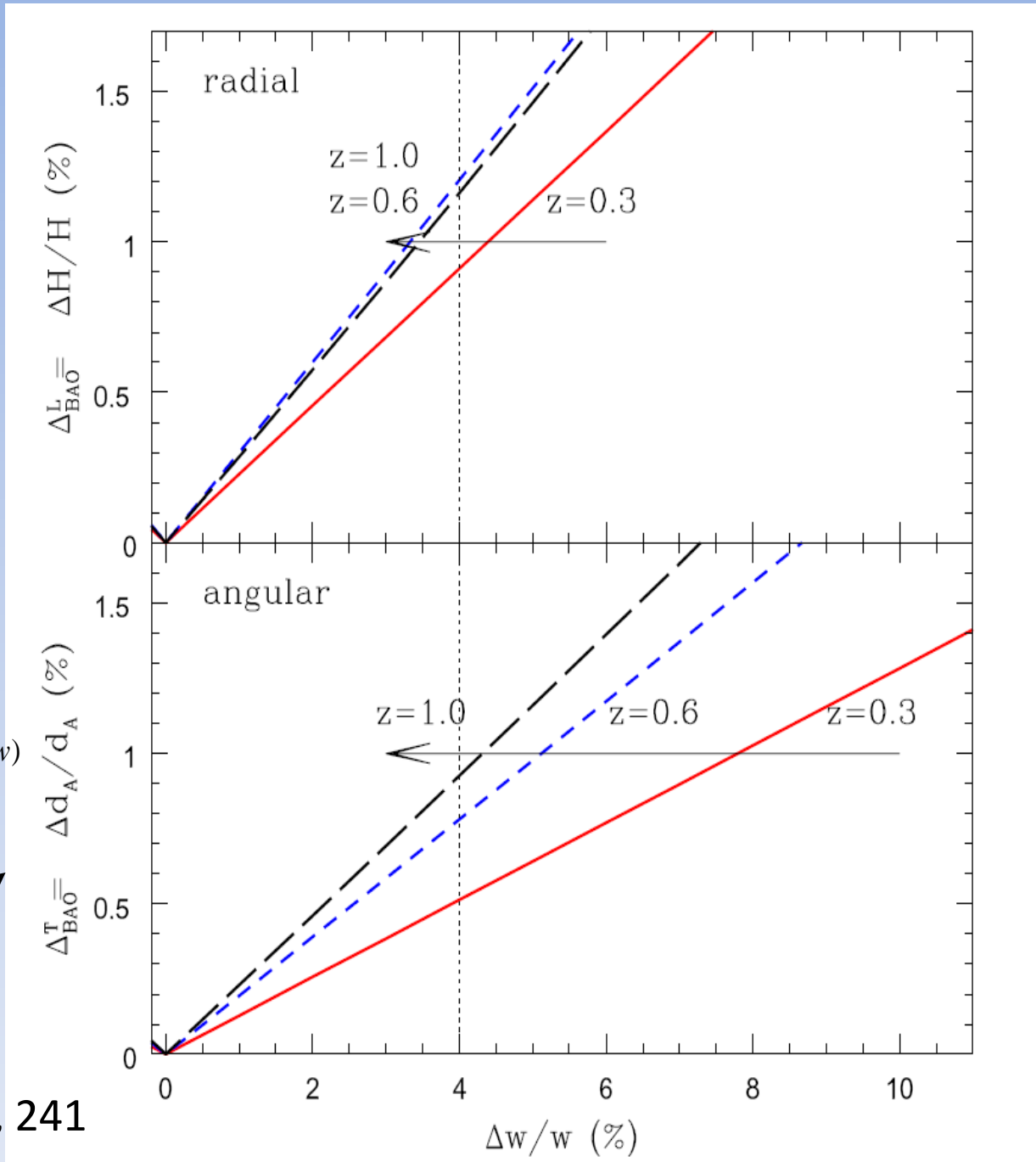
Importance of measuring in the radial direction:

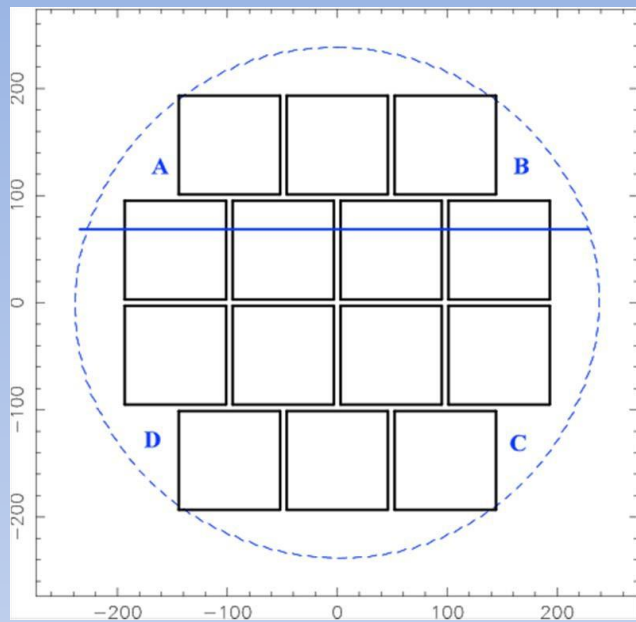
Assume flat universe,
 $w = \text{constant}$ and
 $\Omega_m = .25$

$$\frac{H^2(z)}{H_0^2} = \Omega_m (1+z)^3 + (1-\Omega_m)(1+z)^{3(1+w)}$$

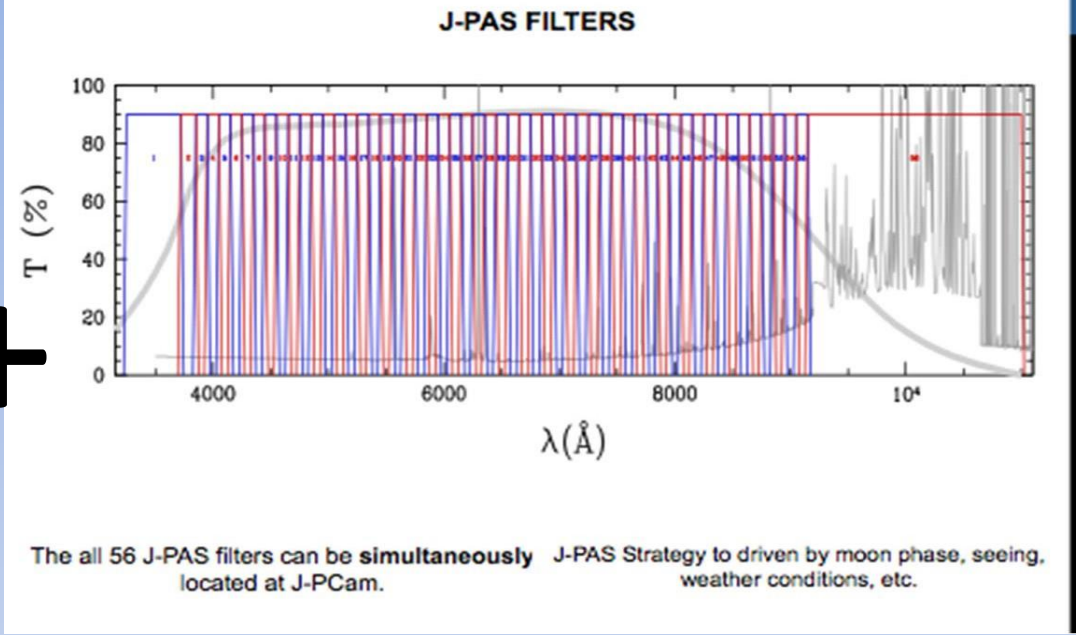
Error propagation:

Benitez et al. 2009 ApJ, 691, 241





+

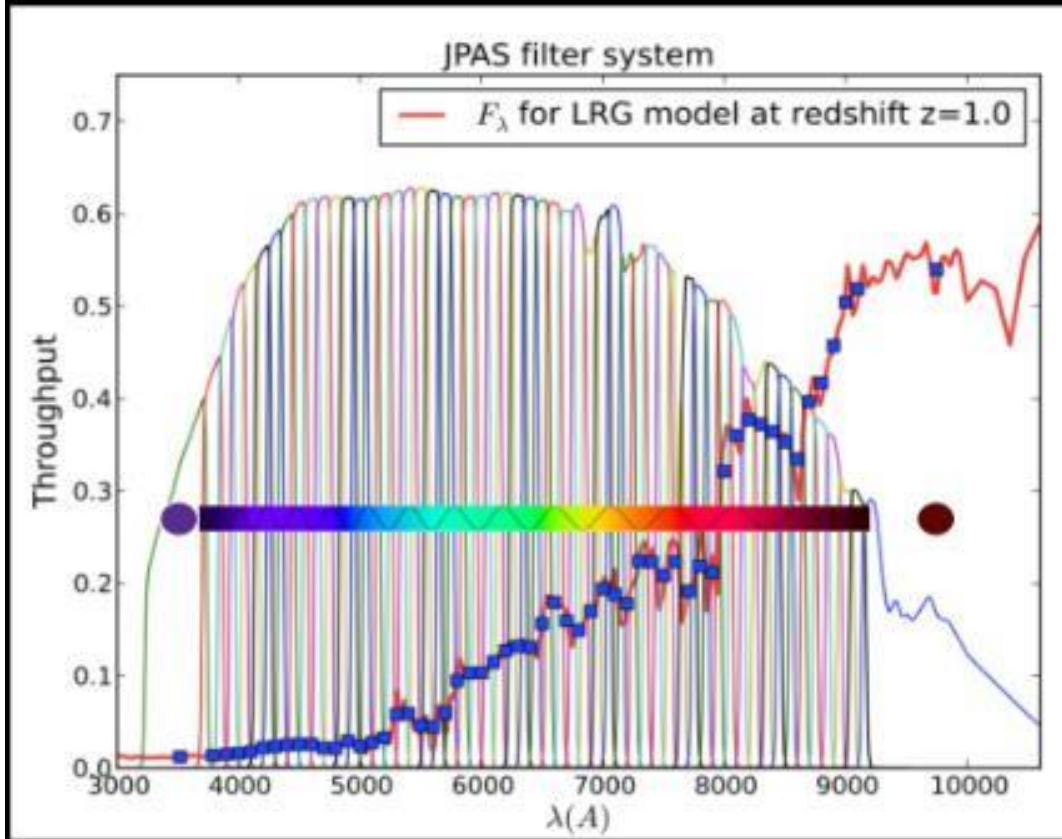


Equivalent to a ~5000/ multiplex spectrograph

- A full system of NB filters has an effective throughput smaller than spectrographs but that is compensated by their stupendous multiplexing **IF** the FOV is large enough
- To surpass the efficiency of state-of-the art spectrographs, the camera size must be very large, >4 sq.degs
- But still costs an order of magnitude less than comparable spectrographs

J-PAS

JAVALAMBRE PHYSICS OF THE ACCELERATED UNIVERSE ASTROPHYSICAL SURVEY DEFINITION & IMPLEMENTATION



8500 deg² (14Gpc³)

- 54 NB Filters (FWHM~14.5nm; $\Delta\lambda\sim 10\text{nm}$)
- 1 Blue MB filter (FWHM~260Å; $\lambda_c\sim 3600\text{\AA}$)
- 1 Red BB filter (FWHM~620Å; $\lambda_c\sim 9500\text{\AA}$)
- Sloan u, g, r

In ~ 7 years

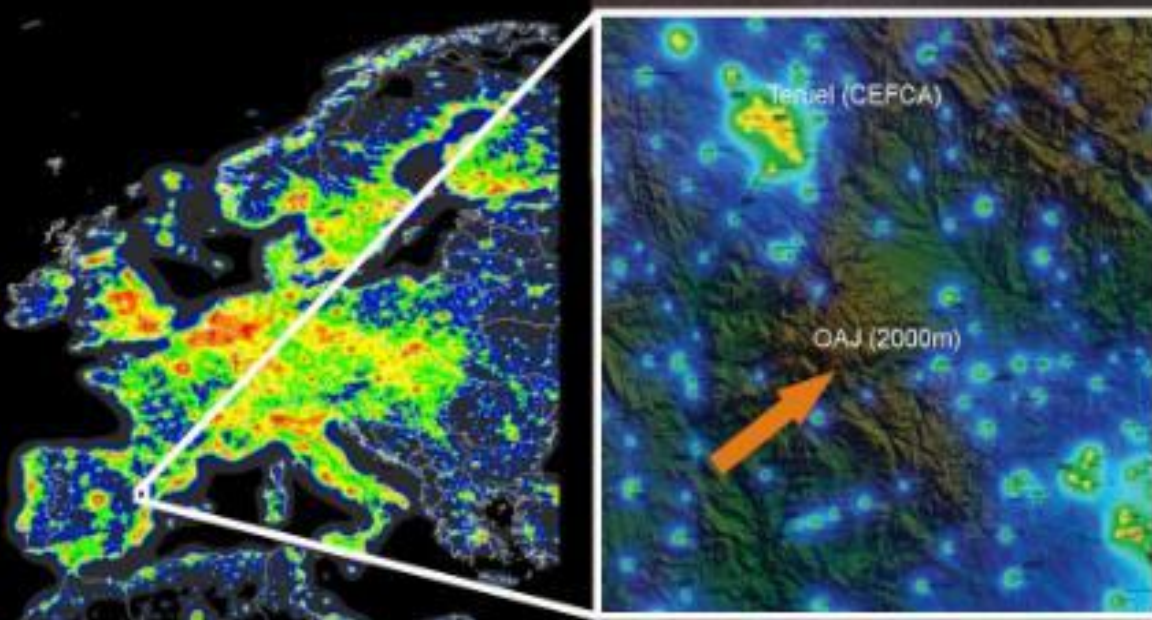
- BAOs: $\delta z / (1+z) < 0.003$
- Weak Lensing, Clusters, SNe

From Javier Cenarro

THE JAVALAMBRE OBSERVATORY (OAJ)

RECOGNIZED IN 2017 AS A "STARLIGHT RESERVE" BY THE STARLIGHT FOUNDATION

$\mu_V \sim 22 \text{ mag/arcsec}^2$
Seeing (median) = 0.71"
Seeing (mode) = 0.58"



From Javier Cenarro



**GOBIERNO
DE ARAGON**



GOBIERNO
DE ESPAÑA

MINISTERIO
DE ECONOMIA
Y COMPETITIVIDAD



OBSERVATORIO ASTROFÍSICO DE JAVALAMBRE OAJ TELESCOPES



DIRECTOR

A. Javier Cenarro
CEFCA
OAJ Project Manager





OAJ

12th J-PAS Meeting
Rio de Janeiro, 11-15 Apr 2016

A. Javier Cenarro



LARGE FOV TELESCOPES AT THE OAJ FOR LARGE SKY SURVEYS

JST/T250

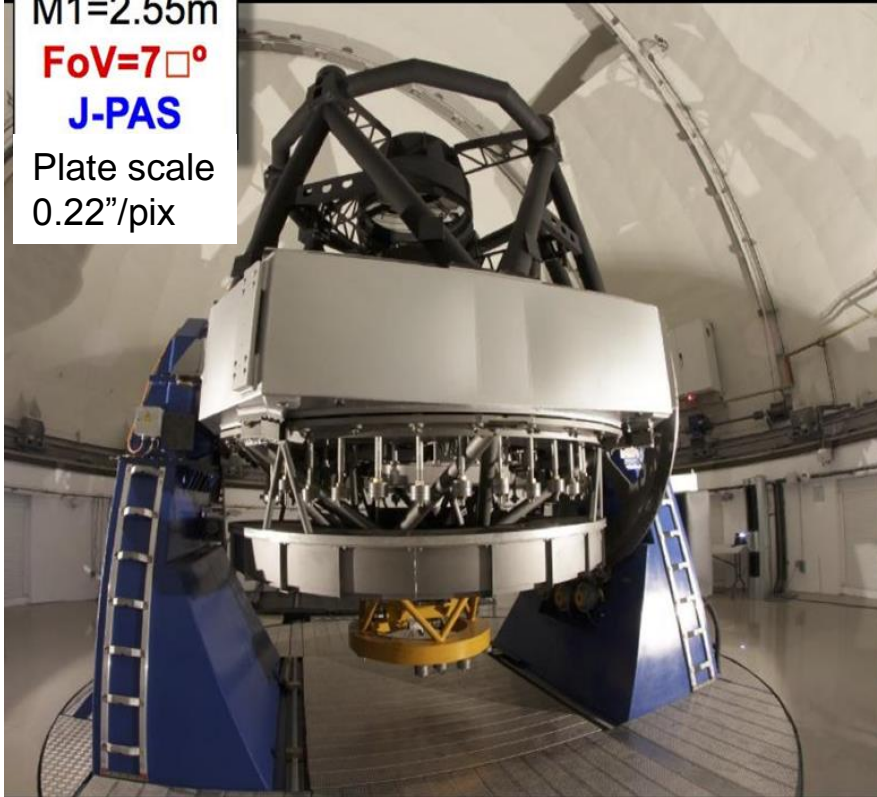
M1=2.55m

FoV=7°

J-PAS

Plate scale

0.22"/pix

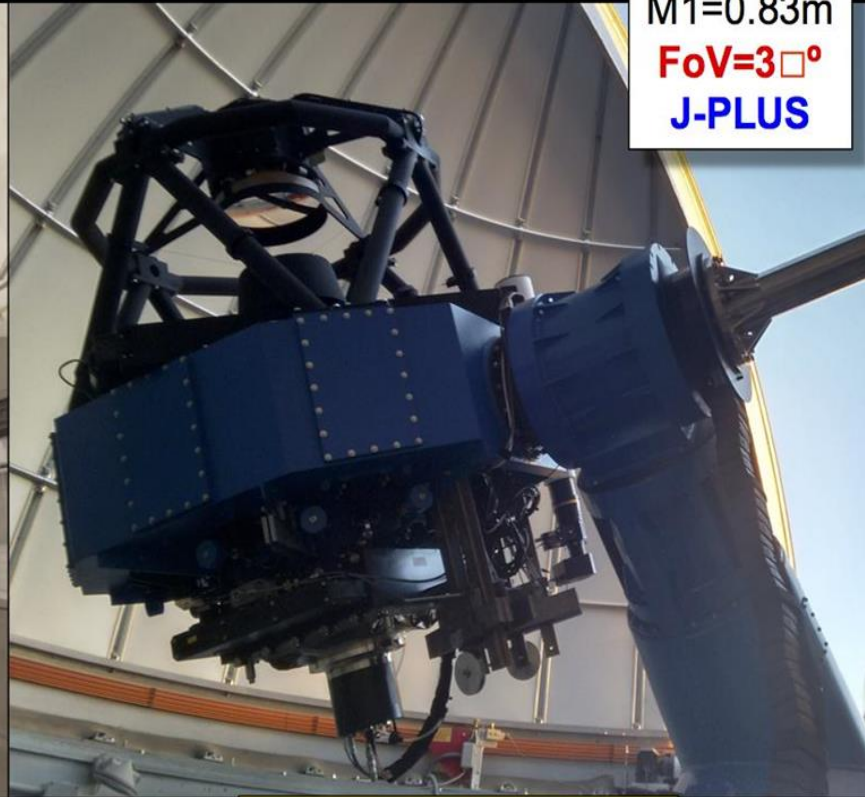


JAST/T80

M1=0.83m

FoV=3°

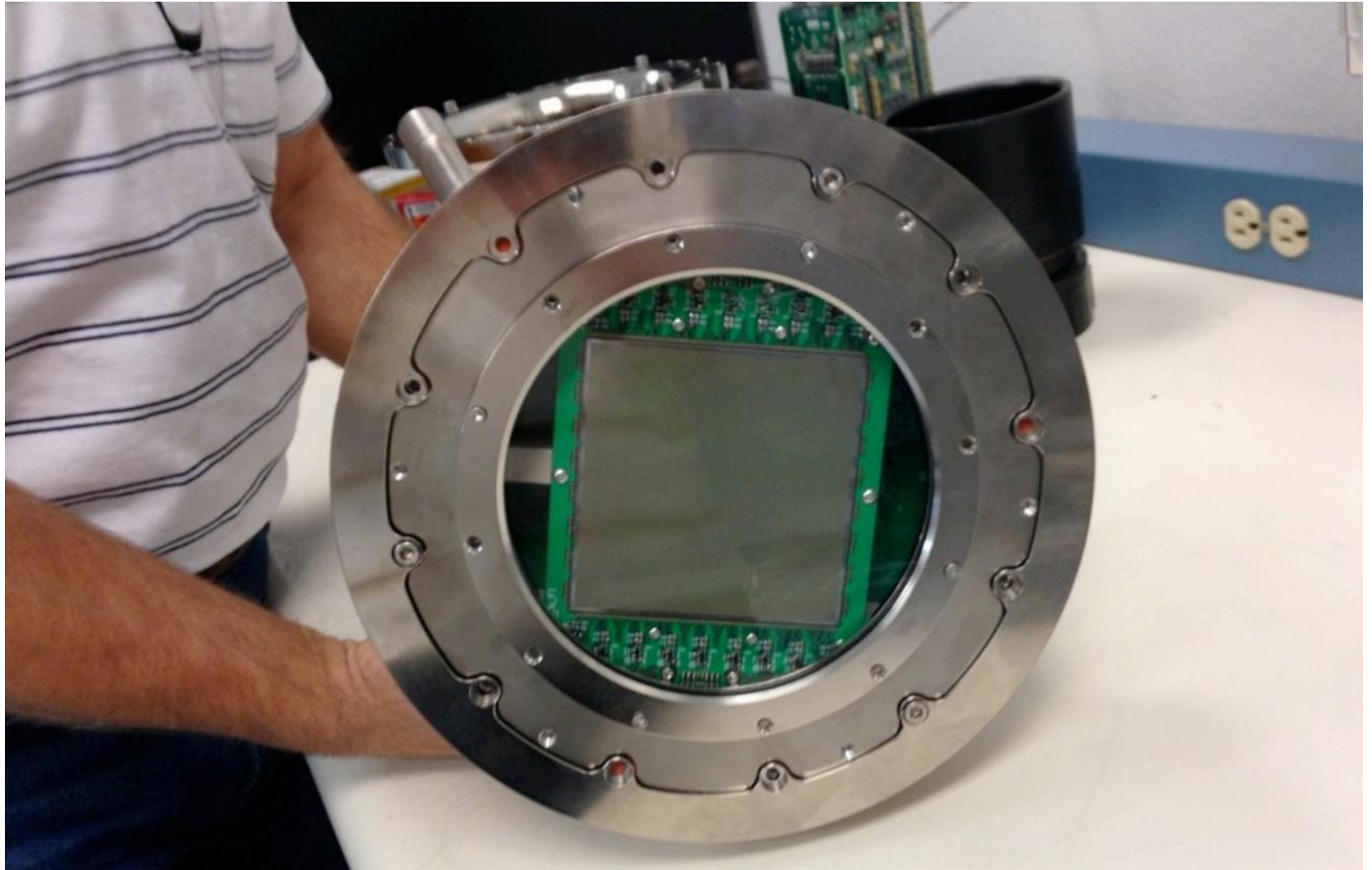
J-PLUS



**Already on site with PathFinder
Commissioning & mini-jpas**

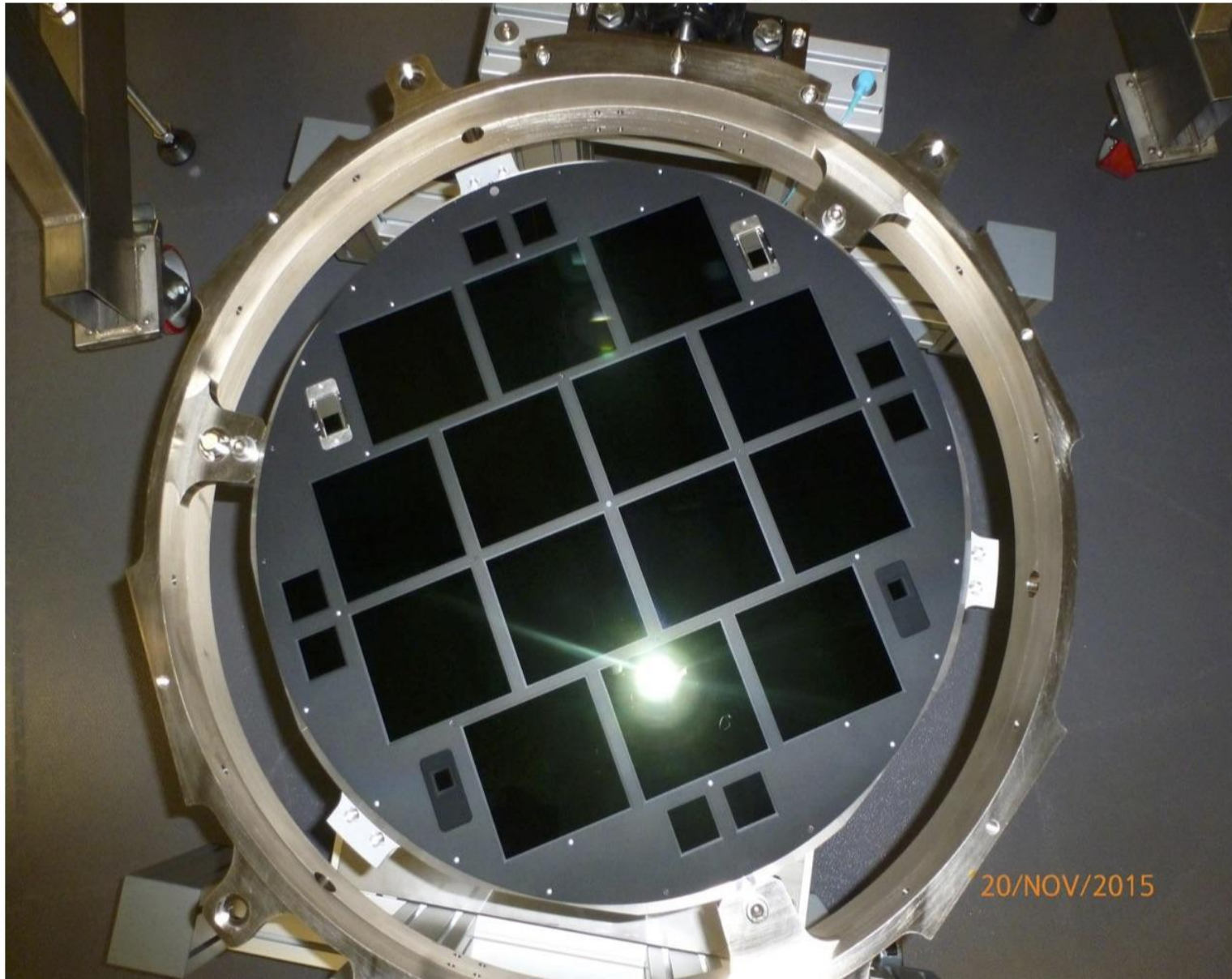
**In science operations
since Nov 2015**

CCD installed in T80Cam – 5/2013
Taking data since 2015



JPCam CryoCam

Grade-5 focal plane assembly (ev2 – Nov'15)



20/NOV/2015

JPCam

FoV	$\varnothing=3.0^\circ$ (full performance) $\varnothing = 3.1^\circ$ (reduced performance)
\varnothing EE50	0.23'' / 10 μm / 1 pix
\varnothing EE80	0.45'' / 20 μm / 2 pix
CCD format	(14 x) 9216 x 9232 pix 10 $\mu\text{m}/\text{pix}$ 1.2 Gpixel camera
Pixel scale	0.23''/pix
Full well	123ke ⁻
Read out time	13.5s
Read out noise	8 e ⁻ /pixel (goal 4e ⁻)
Dark current	0.001e ⁻ /s/pix
FoV coverage	4.7 \square° (fill factor ~70%)
# filters	56 + BB (J-PAS filters)

At 5.6 e- now

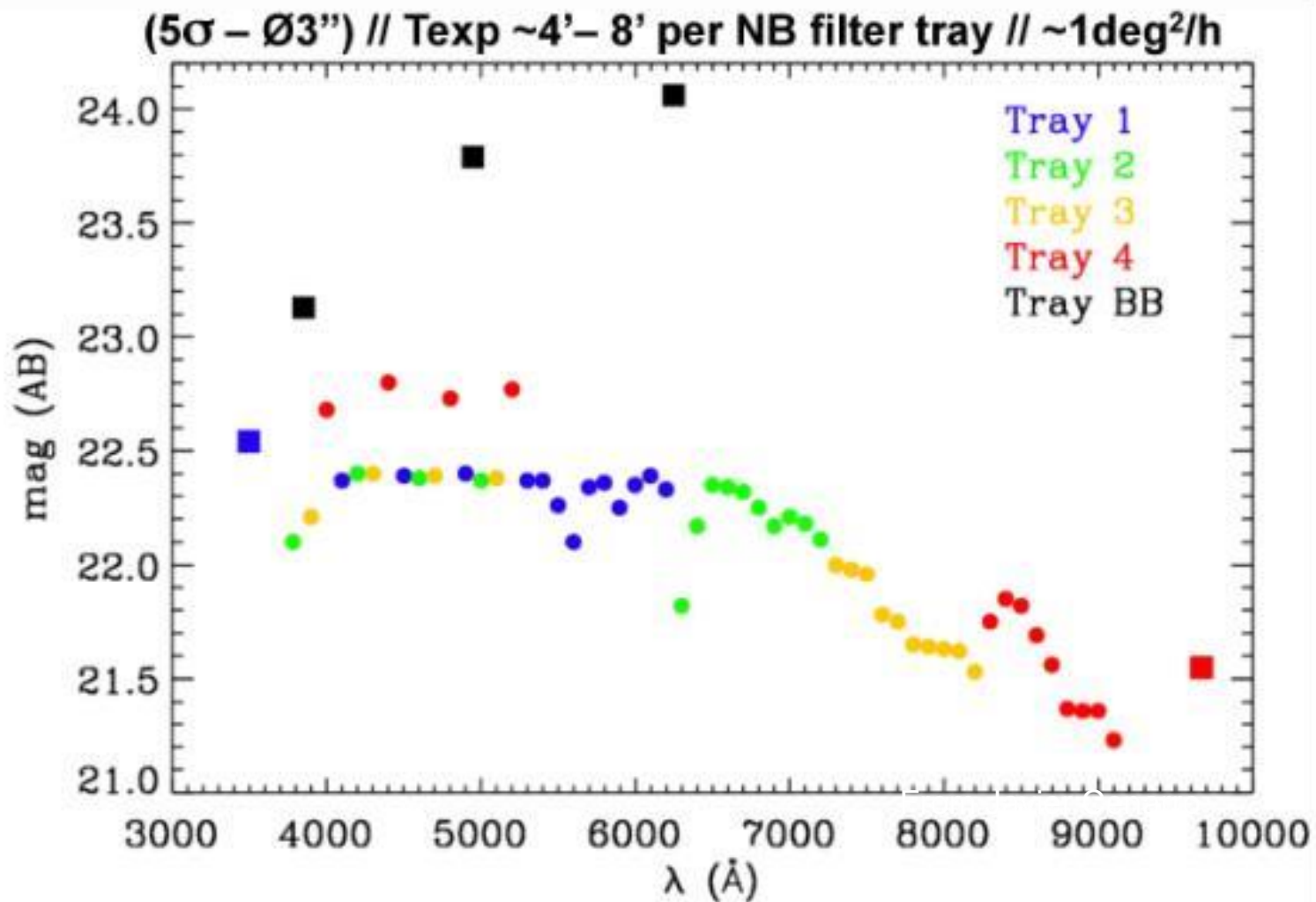
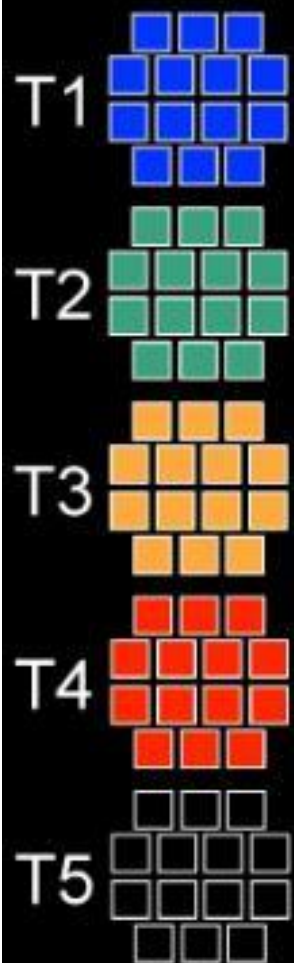
The camera + filters



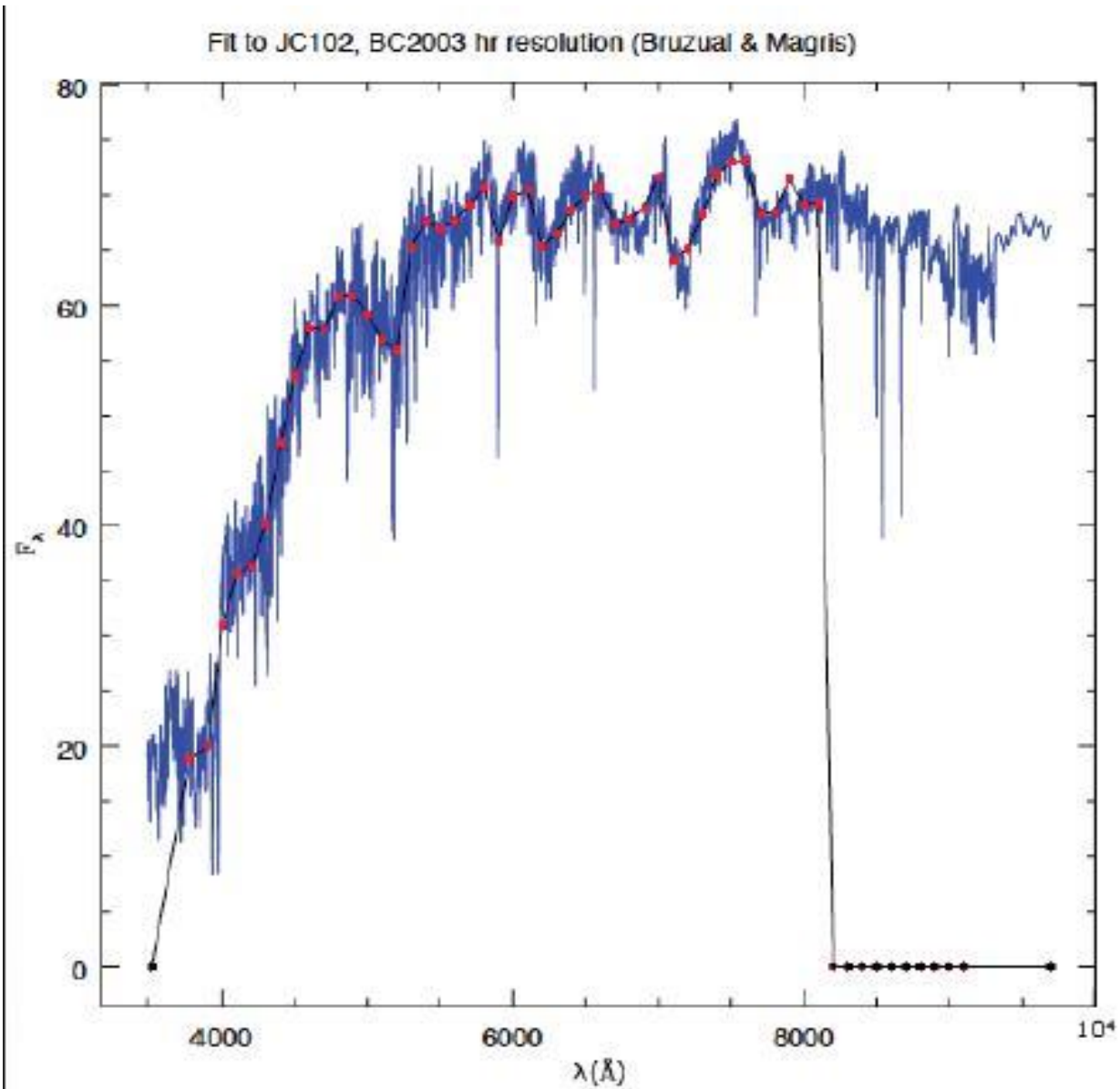
Every CCD “sees” a different filter in each tray x (4+1) trays



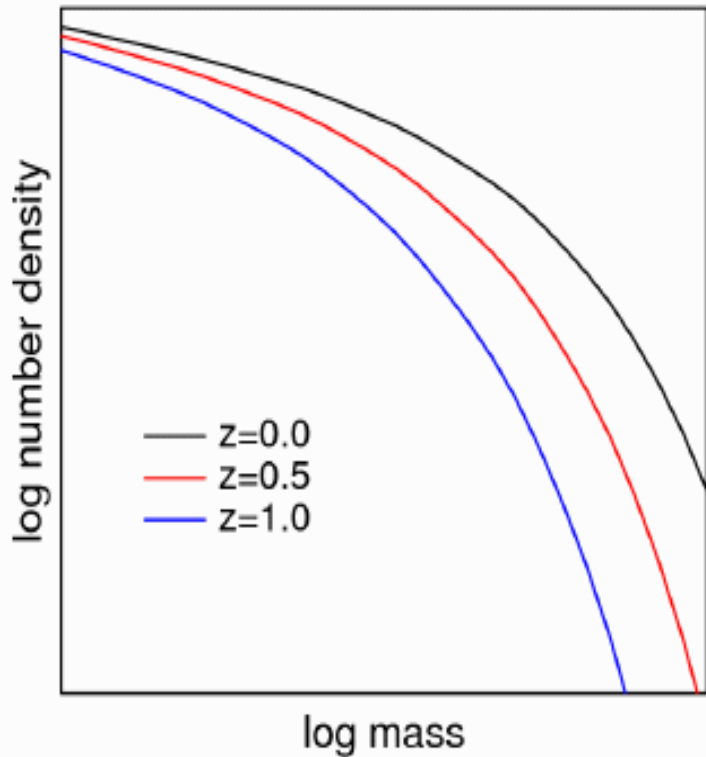
J-PAS LIMITING MAGNITUDES



Not only cosmology: For high S/N objects, it is low resolution spectroscopy

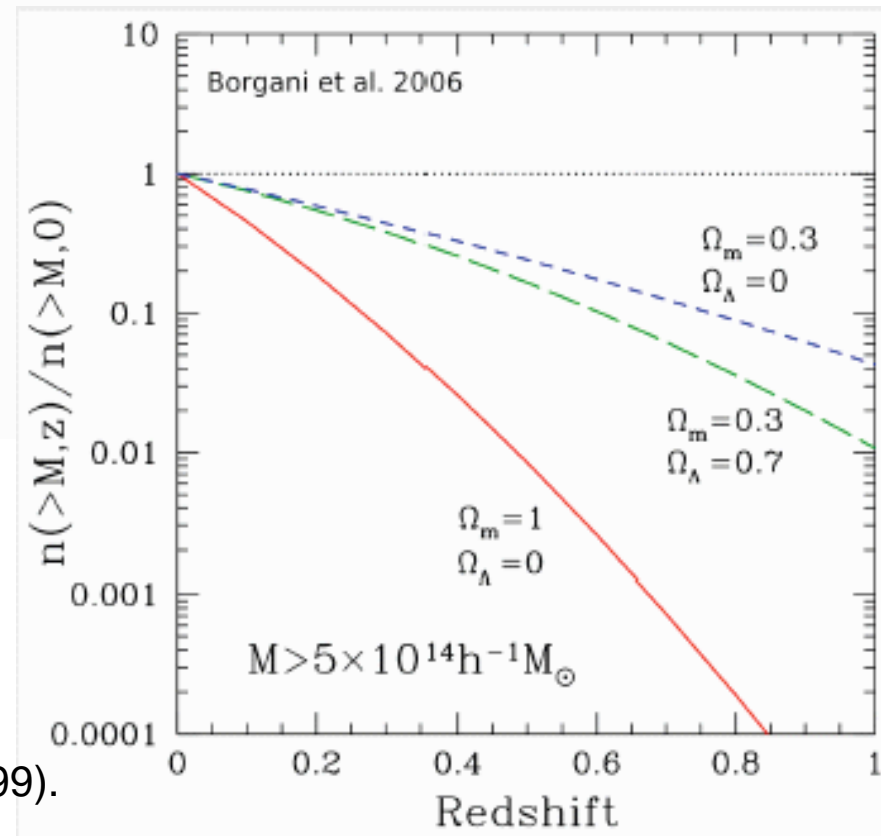


Cluster abundance as a function of mass and redshift probes the mass function and expansion history.

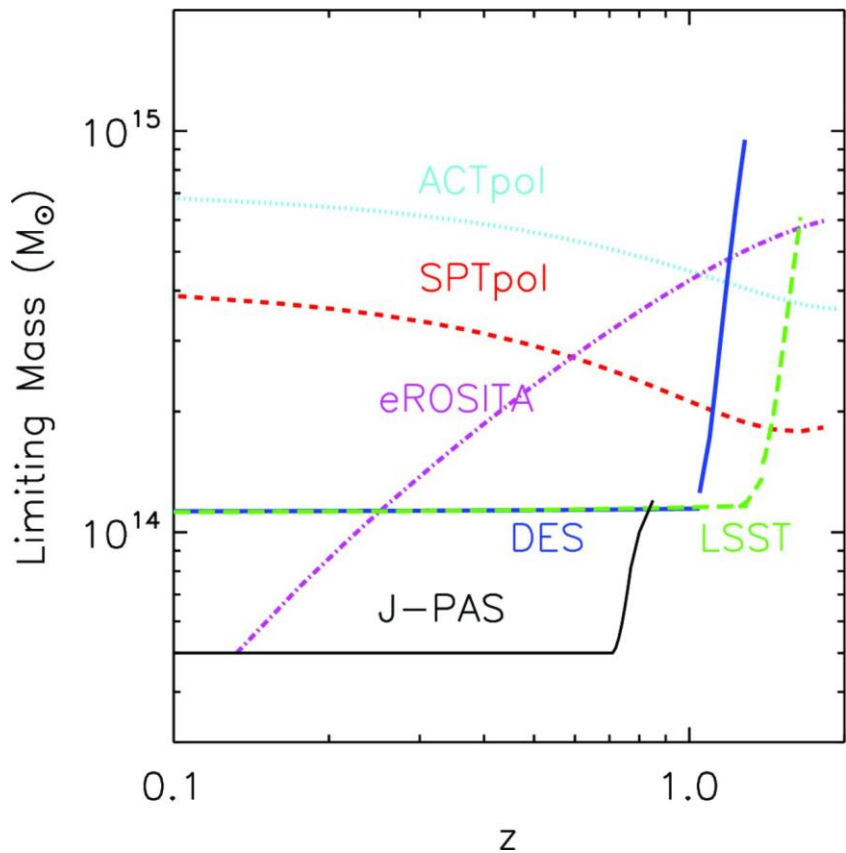


- ▶ Low redshift clusters $\rightarrow \Omega_m, \sigma_8$
- ▶ Evolution \rightarrow dark energy

- Clusters are thought to be “fair samples”.
- If so $f_b \sim \Omega_b/\Omega_m$ (White et al 1993).
- Ω_b comes from Big Bang nucleosynthesis (Schramm & Turner 1998)
- Strong constraints to Ω_m (e.g. Bahcall et al 1999).



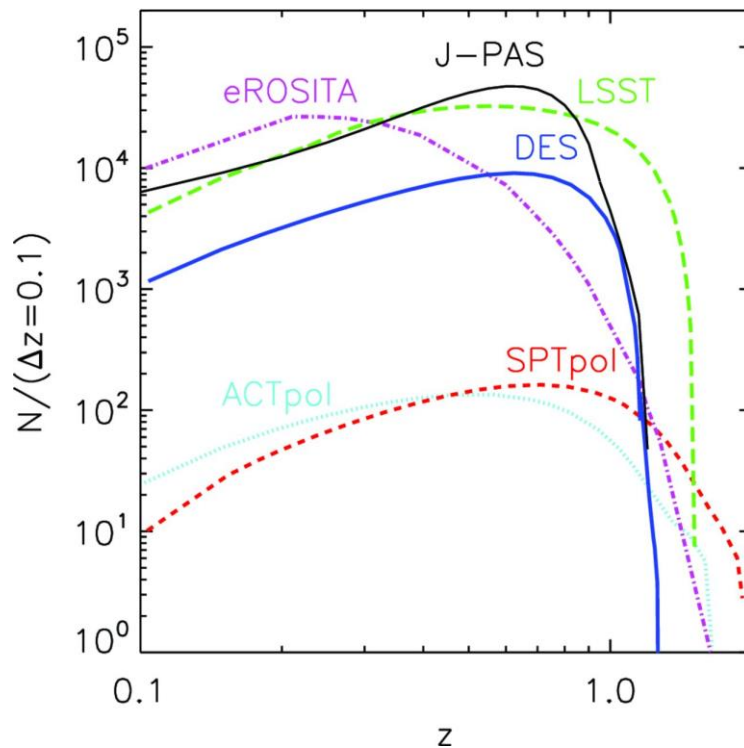
Selection function for different next-generation surveys: J-PAS (black solid line), DES (blue three dot-dashed line), LSST (green long dashed line), SPTpol (red short dashed line) and ACTpol (dotted cyan line).



Because of 100% completeness in redshifts and excellent redshift precision, low mass detection limits are extremely low
 Note that we arbitrarily stop at 4×10^{13} ...

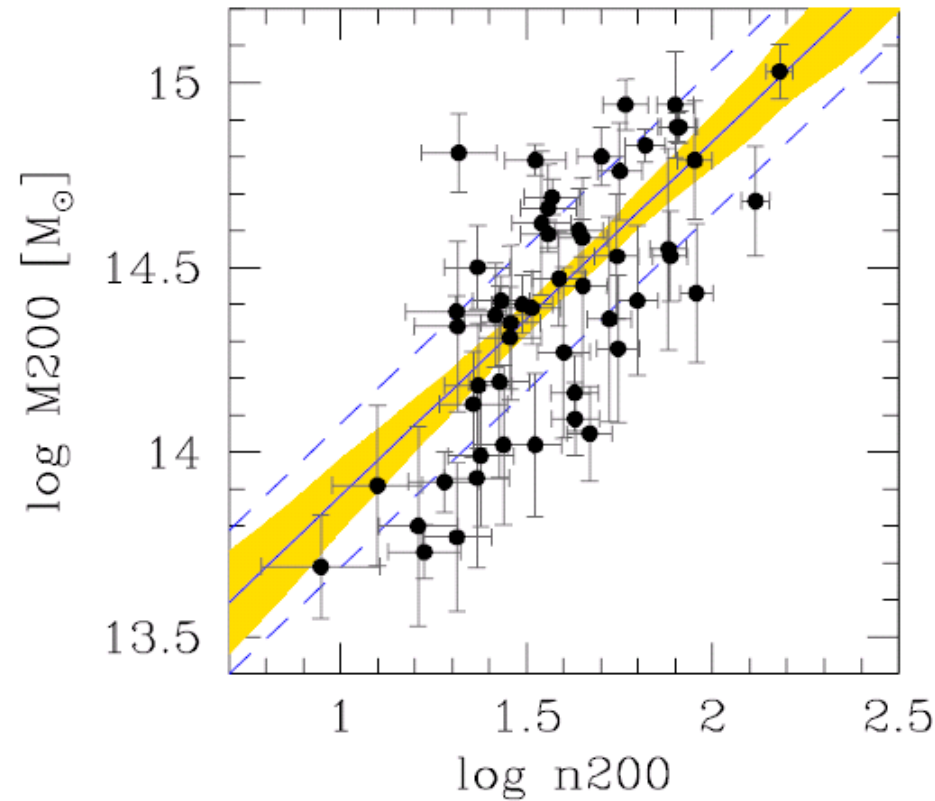
Ascaso, Benitez , Dupke & J-PAS col 2015

Total number of groups/clusters per redshift bin as a function of redshift for different next-generation surveys: J-PAS (black solid line), DES (blue three dot-dashed line), LSST (green long dashed line), SPTpol (red short dashed line) and ACTpol (dotted cyan line).

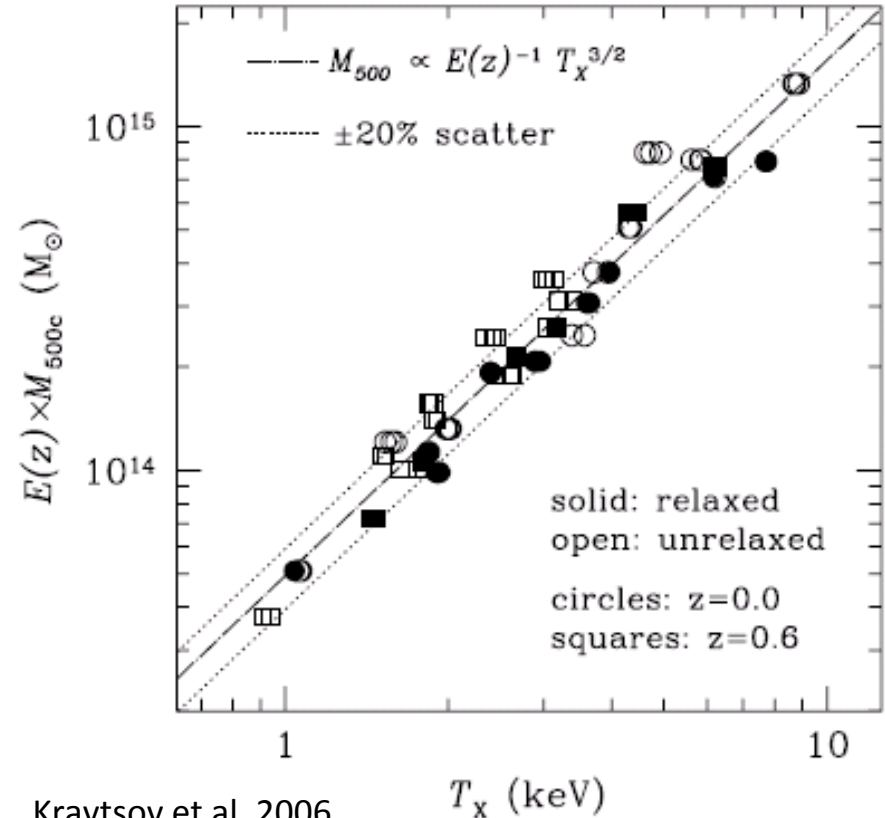


Clusters of Galaxies

- Mass Proxies -

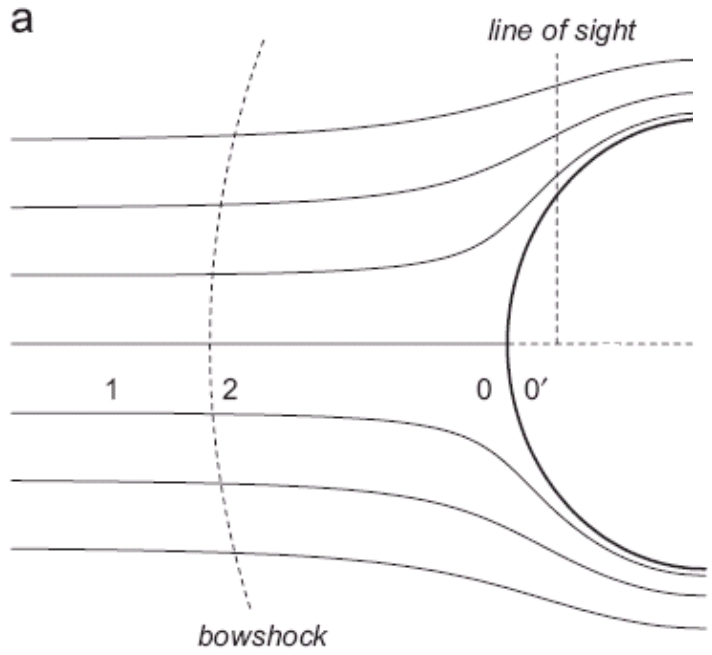
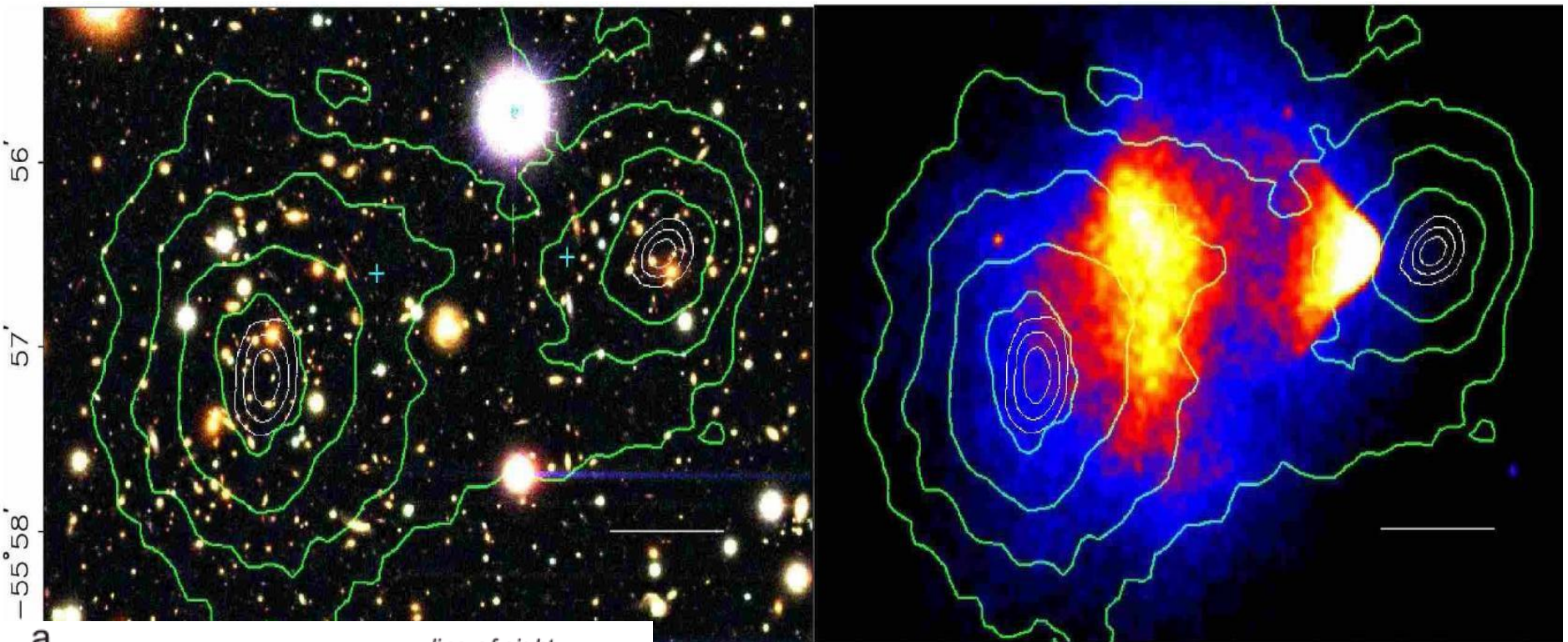


Andreon & Hurn 2010



Kravtsov et al. 2006

FIG. 2.—Relation between the X-ray spectral temperature, T_X , and total mass, M_{500} . T_X is measured within the radial range $(0.15-1)r_{500}$. Separate symbols indicate relaxed and unrelaxed clusters, and also $z=0$ and 0.6 samples. The dashed line shows the power-law relation with the self-similar slope fitted to the entire sample, and the dotted lines indicate 20% scatter. [See the electronic edition of the

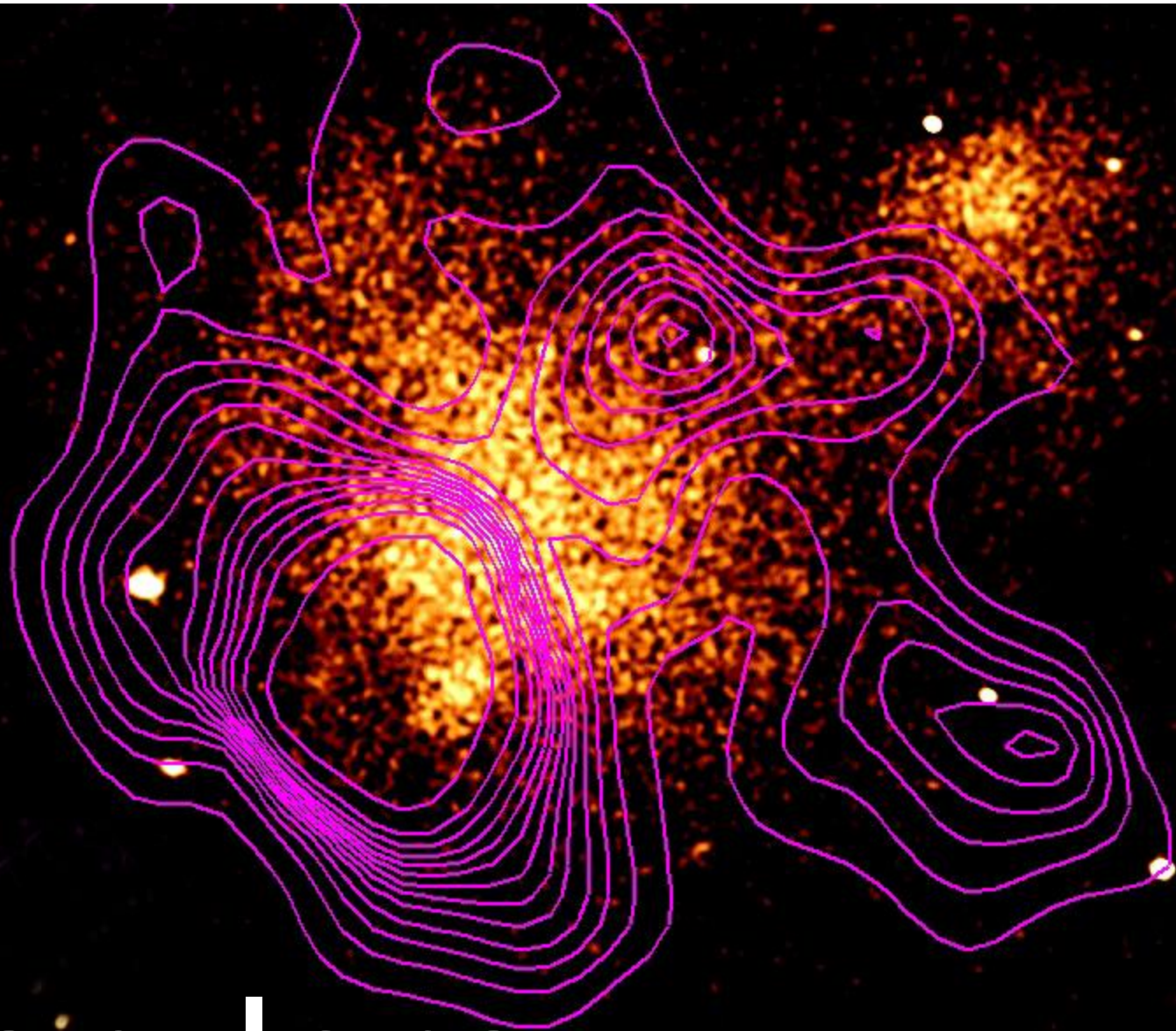


$$\frac{p_0}{p_1} = \left(1 + \frac{\gamma-1}{2} M_1^2 \right)^{\frac{\gamma}{\gamma-1}}, \quad M_1 \leq 1$$

$$\frac{p_0}{p_1} = \left(\frac{\gamma+1}{2} \right)^{\frac{\gamma+1}{\gamma-1}} M_1^2 \left[\gamma - \frac{\gamma-1}{2M_1^2} \right]^{-\frac{1}{\gamma-1}}, \quad M_1 > 1,$$

$\sigma/m < 4$, $M \sim 3 \pm 0.4$ (4700 km s^{-1})





Pandora

Cluster masses

Euler's Equation

$$\underbrace{\frac{\partial \bar{V}}{\partial t} + (\bar{V} \nabla) \bar{V}}_{0?} = -\frac{\nabla P}{\rho} + \bar{g}$$

$$M(< r) = \frac{-kTr}{\mu m_p G} \left(\frac{d \ln T}{d \ln r} + \frac{d \ln \rho}{d \ln r} \right) - \frac{V_r^2 r}{G} \left[\frac{d \ln \rho}{d \ln r} + \frac{d \ln V_r^2}{d \ln r} + 2 \left(1 - \frac{V_\tau^2}{V_r^2} \right) \right]$$

$$\epsilon^{ff} = 1.4 \times 10^{-27} T^{1/2} n_e n_i Z^2 \text{ erg s}^{-1} \text{ cm}^{-3}$$

Usually some variant of King profile to fit the surface brightness

De-projection of lensing masses increases the scatter around the true masses by more than a factor of two due to cluster triaxiality. X-ray mass measurements have much smaller scatter (about a factor of two smaller than the lensing masses) but they are generally biased low by 5-20%. This bias is entirely ascribable to bulk motions in the gas of our simulated clusters. Meneghetti, Raisa et al. 2006, 2009 -estimates a 5-20% error in Mass from this. Nagai more recently 5-10%

Potential for Discriminating mergers with ICL

Jimenez-Teja & Dupke 2016,2017,2018

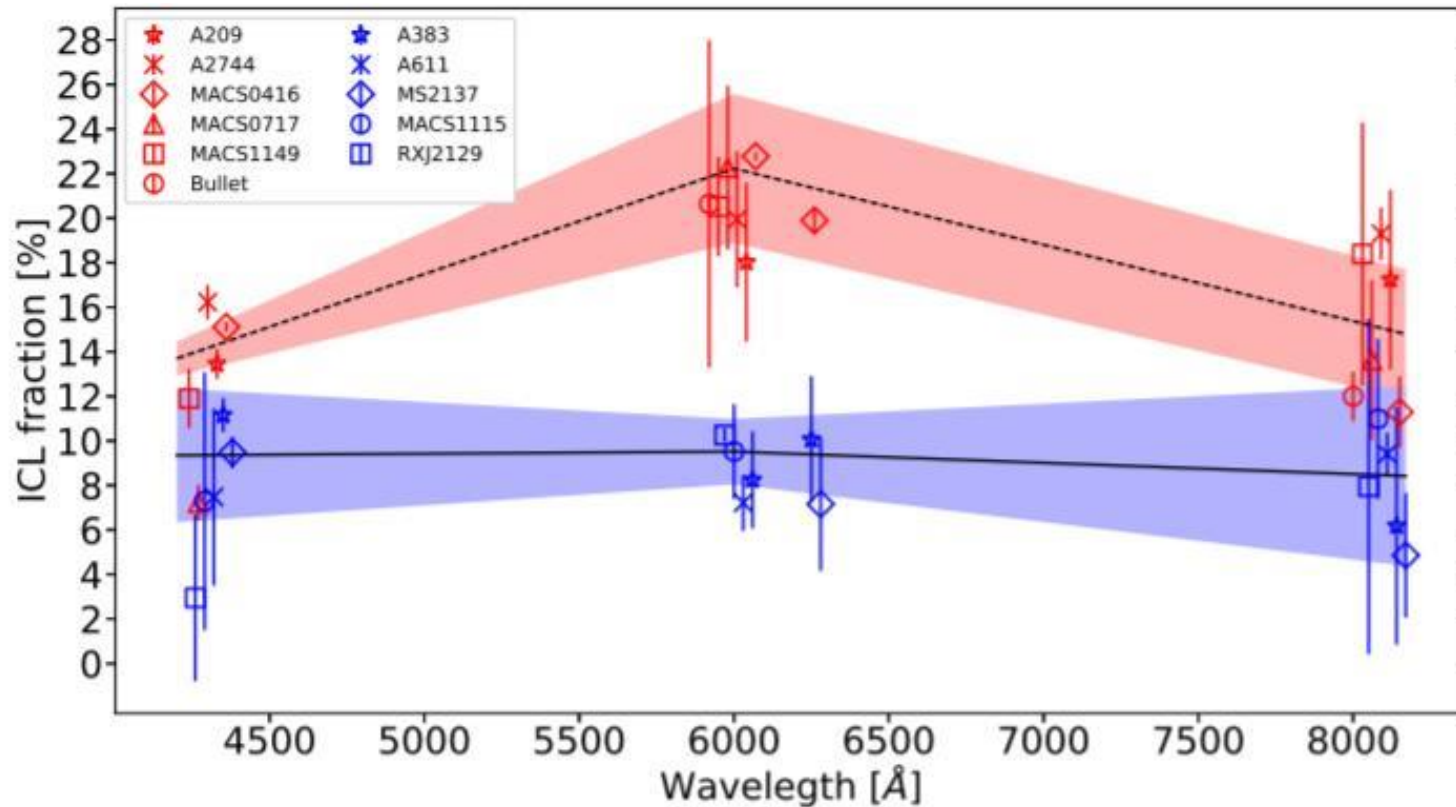


Figure 1. ICL fractions yielded by CICLE for our sample of eleven clusters. Red markers represent merging clusters while blue markers are associated to relaxed systems. The black lines indicates the error weighted mean for each subsample (solid for relaxed clusters and dashed for merging systems), and the shaded areas represent the mean of the errors. For clarity, we have offset horizontally the points by 30 Å gaps.

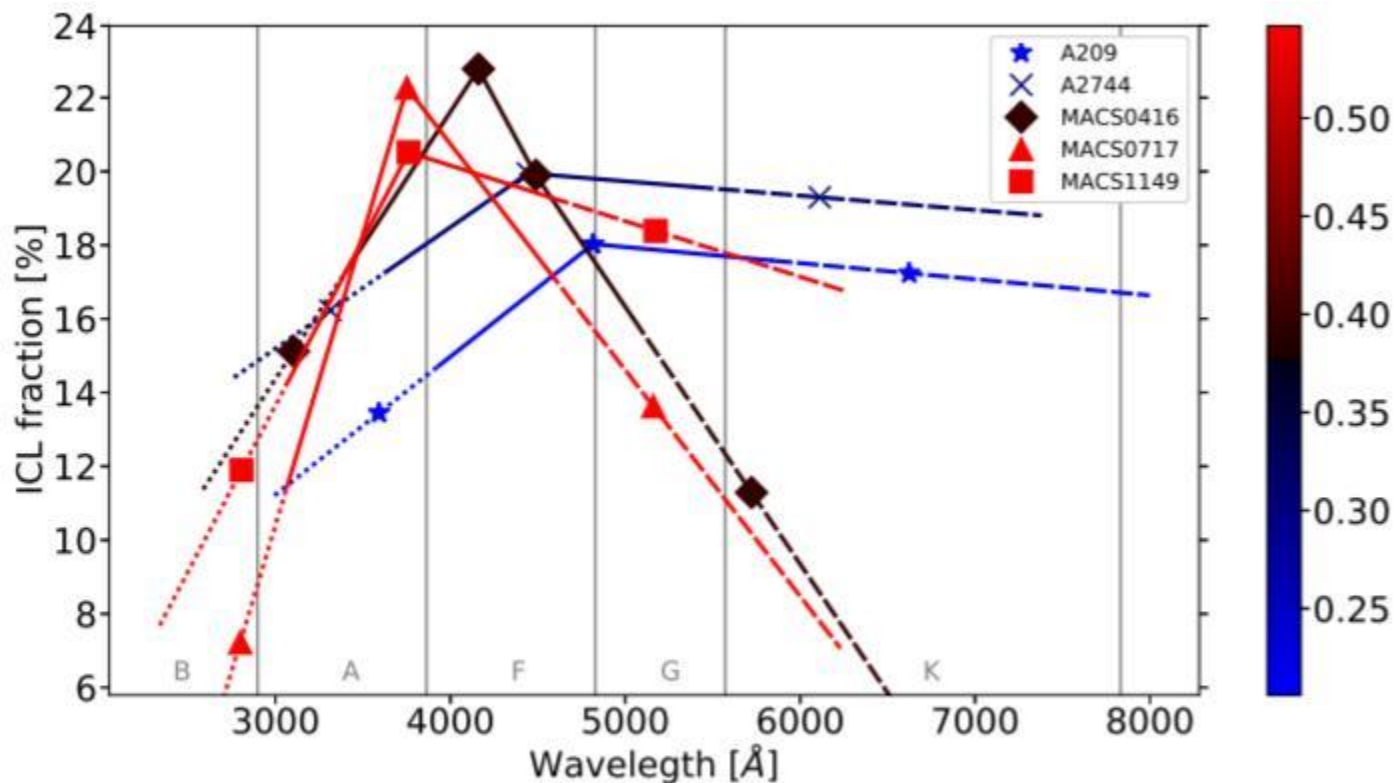


Figure 2. ICL fractions yielded by CICLE for our subsample of merging clusters at rest-frame wavelength. Lines are color coded by redshift and different styles are used to represent the wavelength range covered by each one of the three filters: dotted for the F435W filter, solid for the F606W filter, and dashed for the F814W filter. Vertical gray lines separate the wavelength intervals where the emission peaks of the different stellar spectral types are included, as indicated at the bottom of each region.

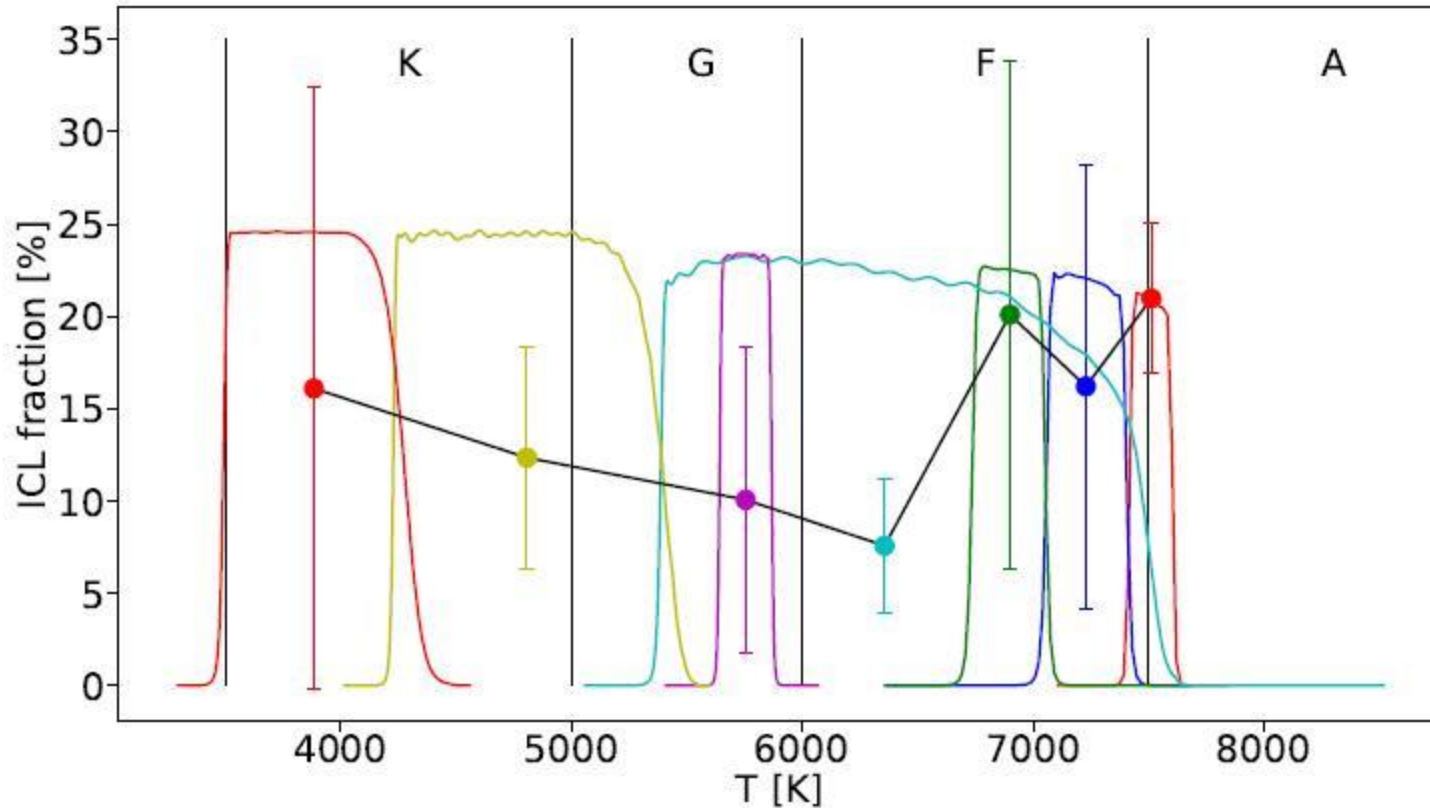
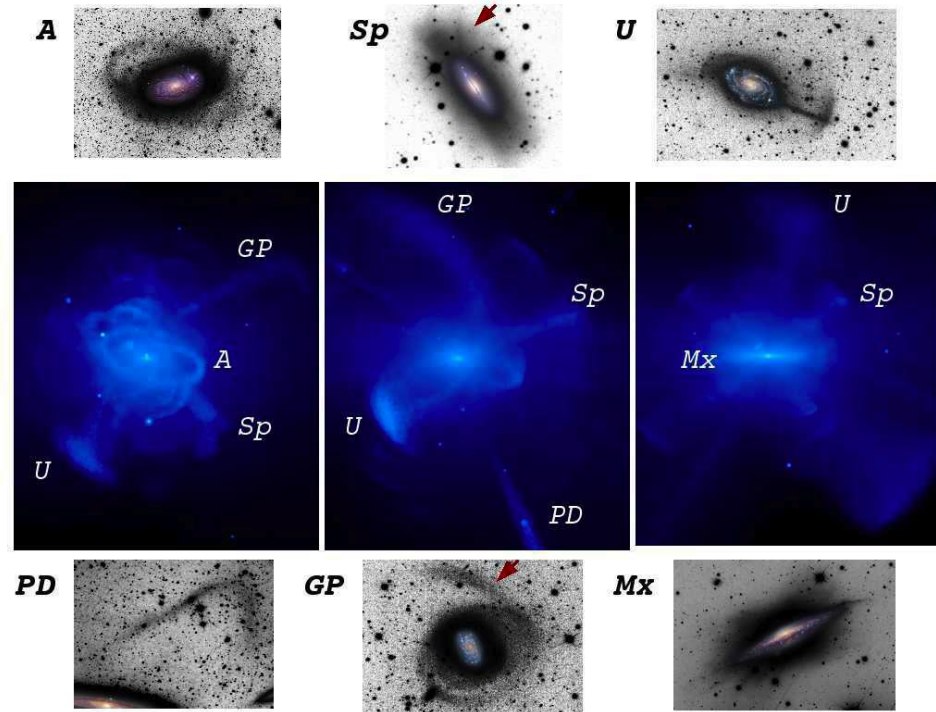


Fig. 1. ICL fractions for Coma as a function of the temperature range covered by each J-PLUS filter. Transmission curves of the seven J-PLUS filters analyzed are shown with lighter solid lines. Vertical black lines delimit the temperature intervals associated to each spectral type.

J-PAS stellar content

RR Lyrae, WD, CV $\rightarrow \sim 200 \times 10^6$
Old, low-mass stars of different nature
WDs, emission-line objects, Carbon stars, etc
Globular clusters
Streams
Halo itself



Galaxy Evolution

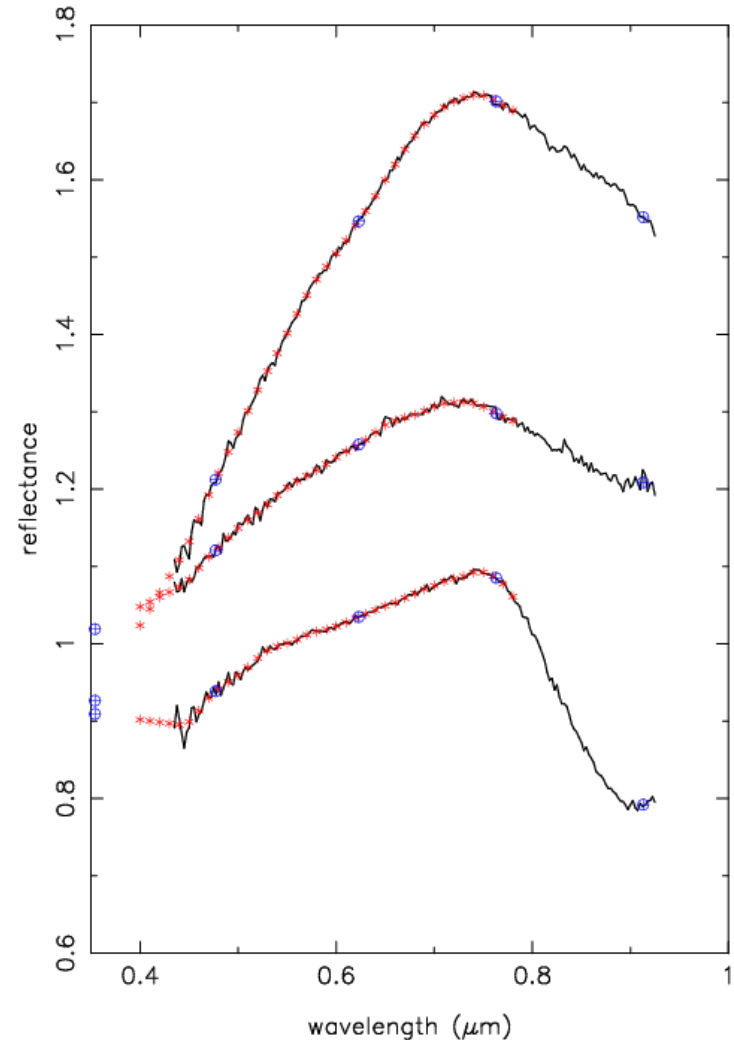
$>10^8$ gals will allow extensive studies of integrated stellar populations down to $z \sim 0.9$ to study galaxy evolution.

Detailed studies of SFR, galaxy mergers and chemical evolution. Fine grain binning of galaxy types (morph, spectra, type, environment). Galaxy environment, absorption systems, etc

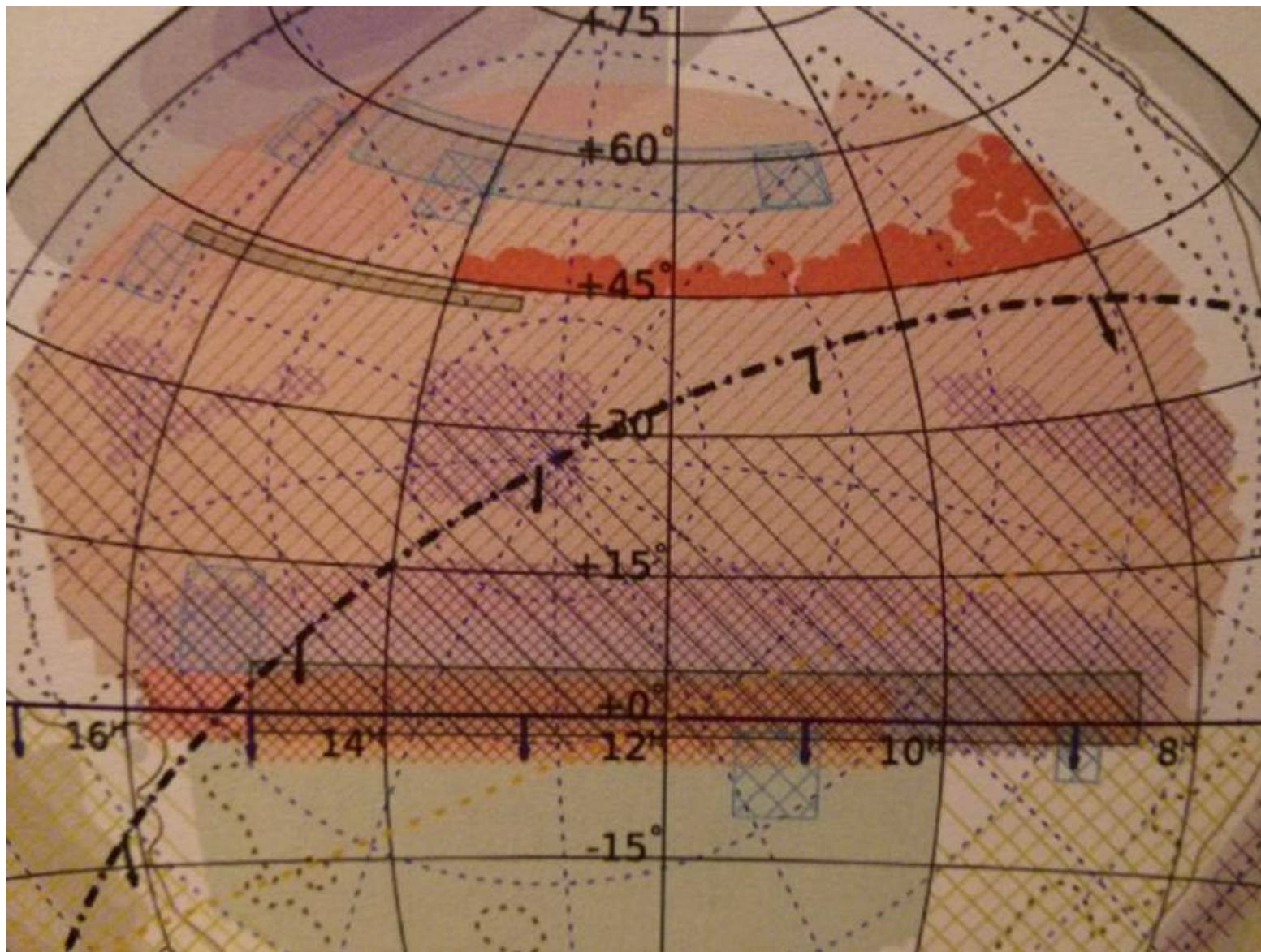
J-Steroids

Asteroid colors opened a window to study their family origin and the chemical distribution in the early solar system.

- 4th release of the SDSS MOC (2008):
 - 220,000 observations of
 - 105,000 asteroids.
- SDSS has a wider spectral coverage
 - Better for OI/Px bands
- J-PAS has a better spectral resolution
 - Ideal for aqueous alteration bands
 - Better for 0.5 μm Steins-like bands



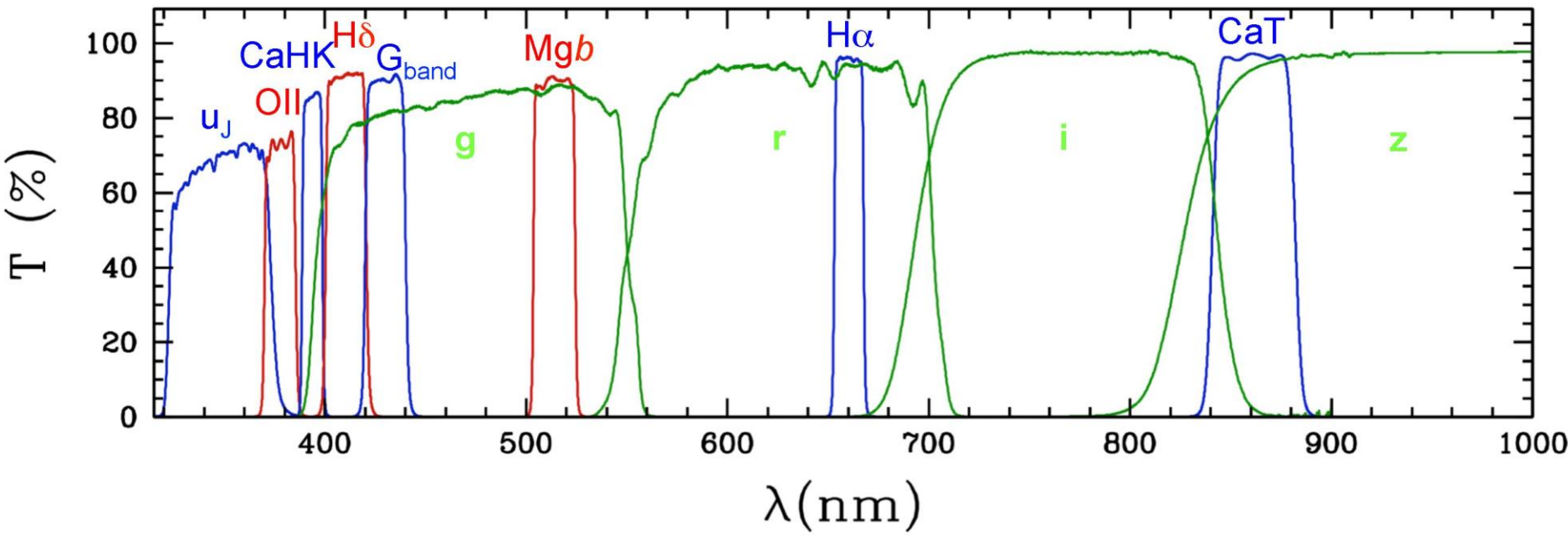
Synergies with WEAVE, EUCLID & Overlap with eROSITA



JPAS = ALL SKY IFU

- JPAS = Javalambre-*Physics of the Accelerated Universe* Astrophysical Survey, Spanish-Brazilian collaboration, PAU-BRASIL is the Brazilian counterpart
- 8500 sq.deg. survey with 54 contiguous filters, 100Å apart $3700\text{Å} < \lambda < 9200\text{Å}$ + 5 broad(er) for lensing. Full coverage $3300\text{Å} < \lambda < 10100\text{Å}$
- Dark site with 0.71 arcsec seeing: Javalambre in Teruel, Spain
- 2.5m tel. + 5 sq.deg. JPCam, 1.2Gpix/shot
- It will measure 0.3% photo-z for $\sim 100\text{M}$ galaxies (Ellip $z < 1.05$ and EmLine $z < 1.4$)
- $\sim 400\text{-}500$ M galaxies with 3% photo-z,
- \sim few M QSOs with 0.3% photo-z > Measure w all the way to $z=3$
- ~ 0.8 arcsec image of the Northern Sky
- Extremely mass sensitive optical cluster catalog
- Excellent characterization of low-z SN systematics
- A few 1000 SNIe survey, no spectroscopy required
- Pixel-by-pixel low-res spectrum of the whole northern sky up to $m \sim 23 / \text{arcsec}^2$
- It will measure radial BAOs up to $z \sim 1.4 \rightarrow 14 \text{ (Gpc/h)}^3$
- Clusters (10^5), Weak lensing, SN(10^4), QSOs (10^6), Galaxy evolution (10^8), Stars (10^8), Asteroids, etc

OBSERVE THE J-PAS AREA WITH THE 12 J-PLUS FILTERS



“Stellar physical parameters can be recovered with a combination of 10-15 medium and broad band filters with S/Ns ~50”

Bailer-Jones (2000, 2004), Bessell (2005), Jordi et al. (2006)

SDSS (g, r, i, z) + u_j + J378_[OII] + J395_[H+K] + J410_[$H\delta$] + J430_[G-band] + J515_[Mgb-Fe] + J660_[$H\alpha$] + J861_[CaT]

J-PLUS DR1

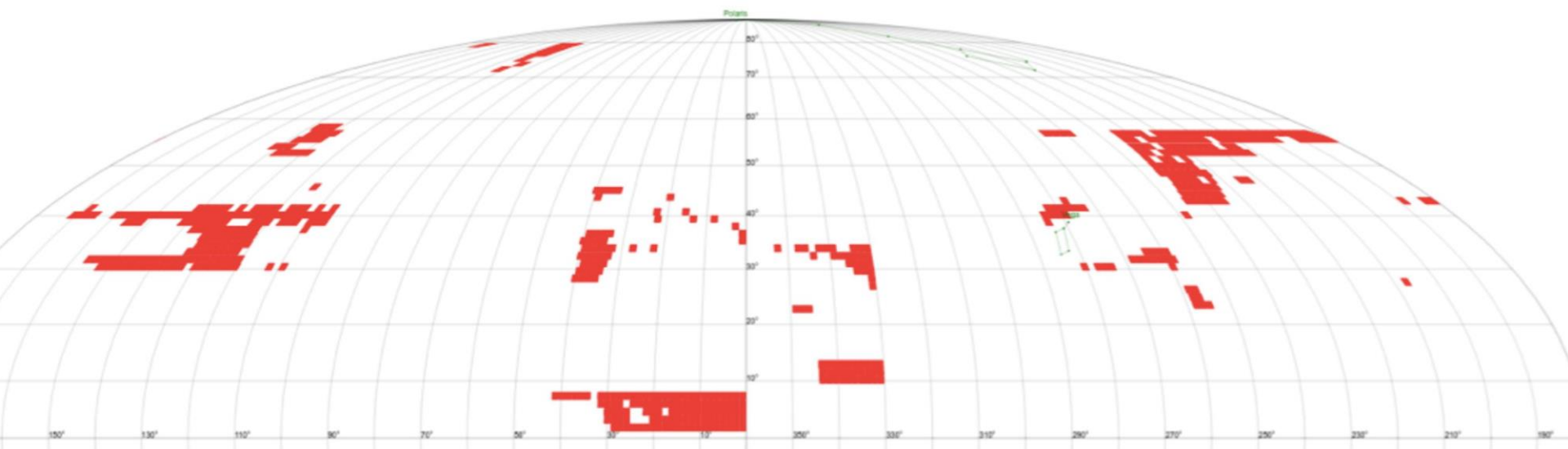


Figure 5: Footprint of the tiles included in J-PLUS Data Release 1.

Sky coverage = 1020 deg^2
4.5M stars + 3M galaxies with $r < 21$

CURRENT STATUS

- **J-PLUS has already >1000 sq deg observed – 36 sq deg public**
- **PathFinder is doing fine and it is expected that Science data started last week.**
- **JPCam on clean room at OAJ on tests and development of FSU integration – Final Installation after PF ends – 2nd semester 2018**

PF potential fields

PATHFINDER SURVEY

Pathfinder camera: 1 single e2V CCD camera (9.2kx9.2k, 0.227 "/ pix), 0.30 sq.deg effective area

Pathfinder Survey: - **mini-JPAS++**

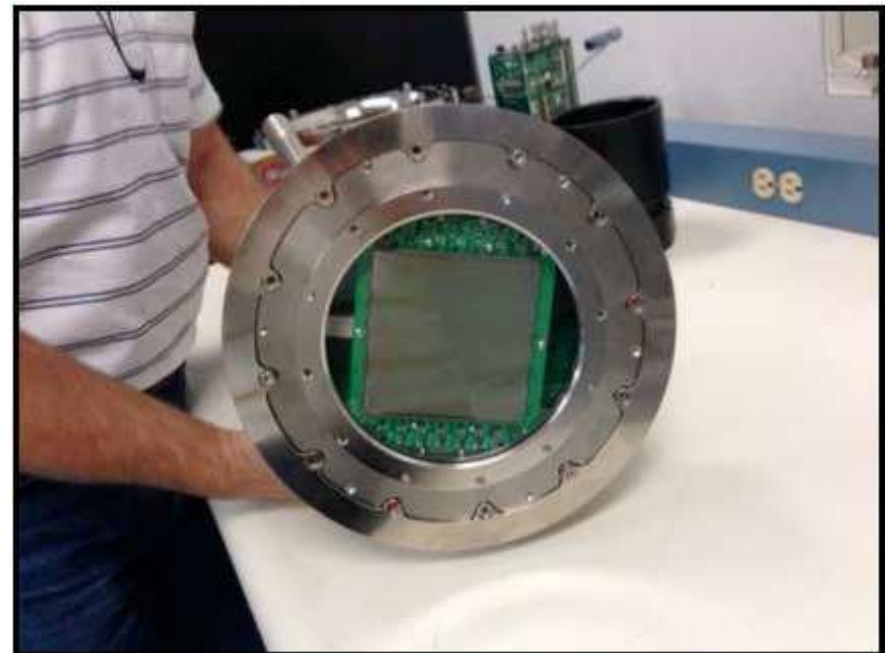
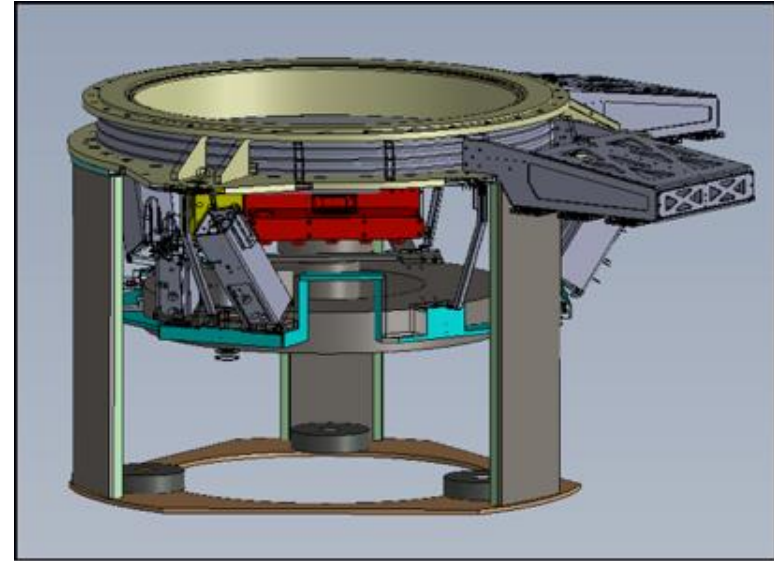
A few sq.deg. covered with 56+ filters to the same depth of the main survey

~10k redshifts with $dz/(1+z) \sim 0.003$

~30k redshifts with $dz/(1+z) = 0.03$

~1000 QSO redshifts

Originaly 2 fields, AEGIS and Hectomap, GAMA (with eROSITA)

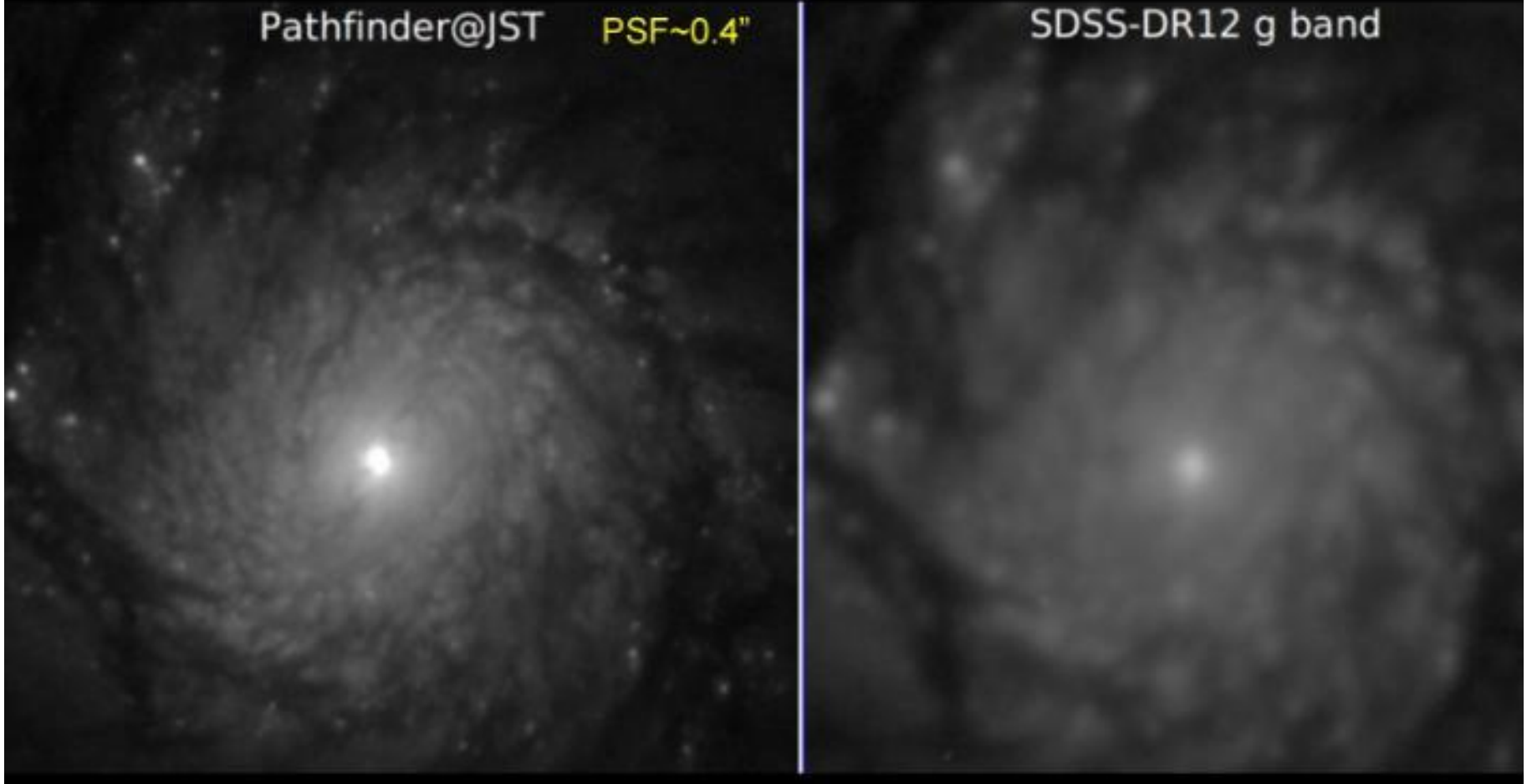


M51, resulting from the combination of 6x10s single exposures with no filter (left), and a g band image from SDSS (right).

JPAS-Pathfinder demonstrates the quality of JST/T250 and the OAJ site

Pathfinder@JST PSF~0.4"

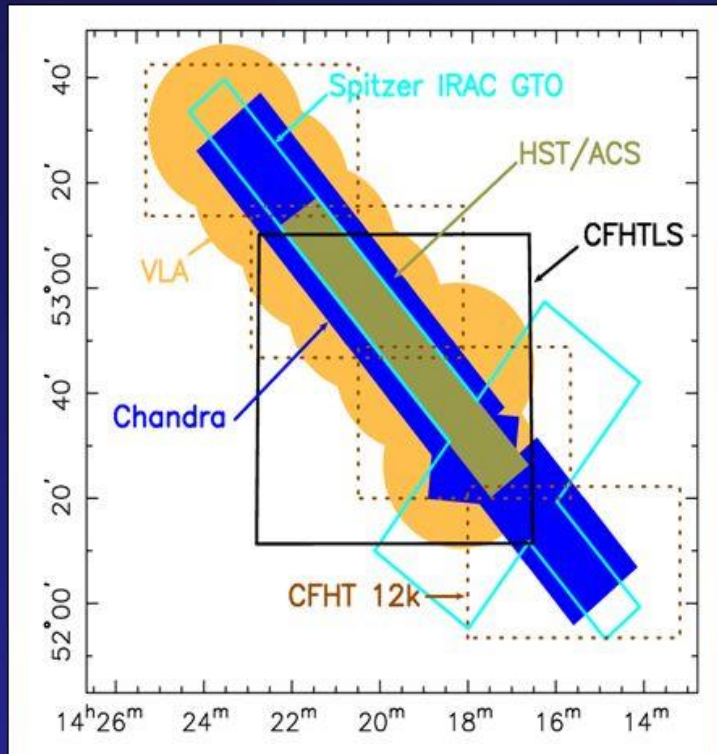
SDSS-DR12 g band



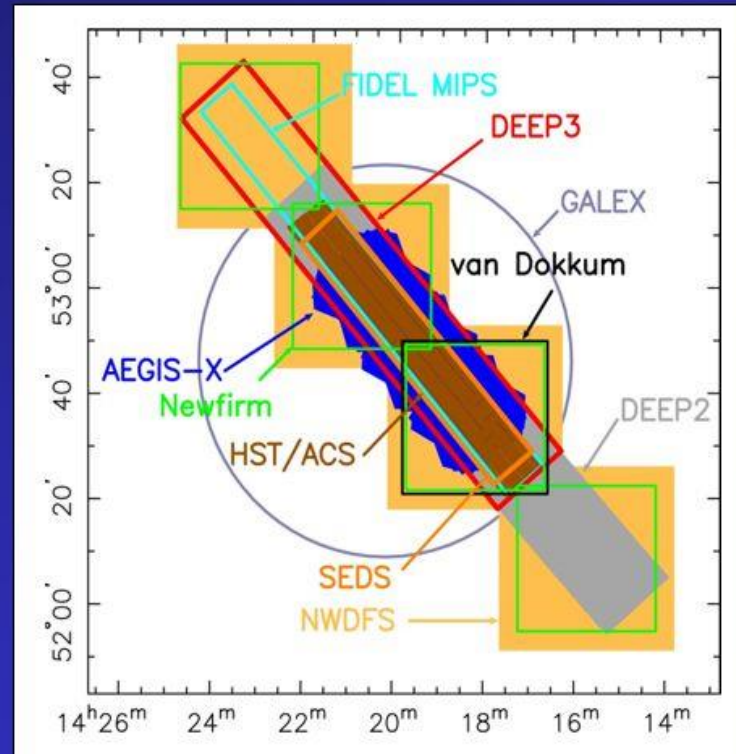
**BEST PRIMARY FIELD aka mini-JPAS field:
AEGIS**

FIELD RA=216.6° Dec=+52.7° Size ~ 1 sq deg

Extended Groth Strip Data Sets



Phase I



Phase II

WHO SCREWED UP THE WEATHER THIS YEAR ??



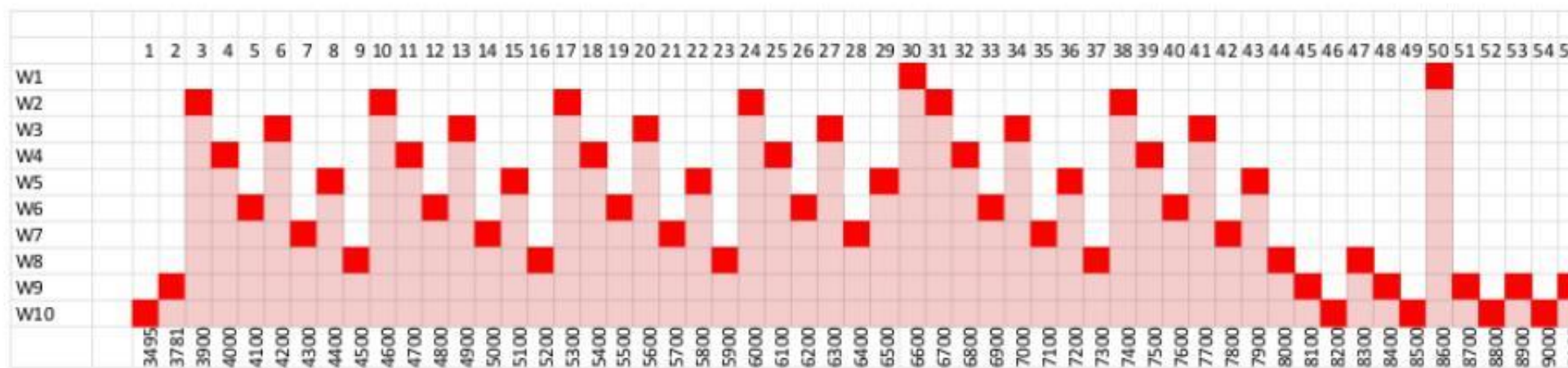
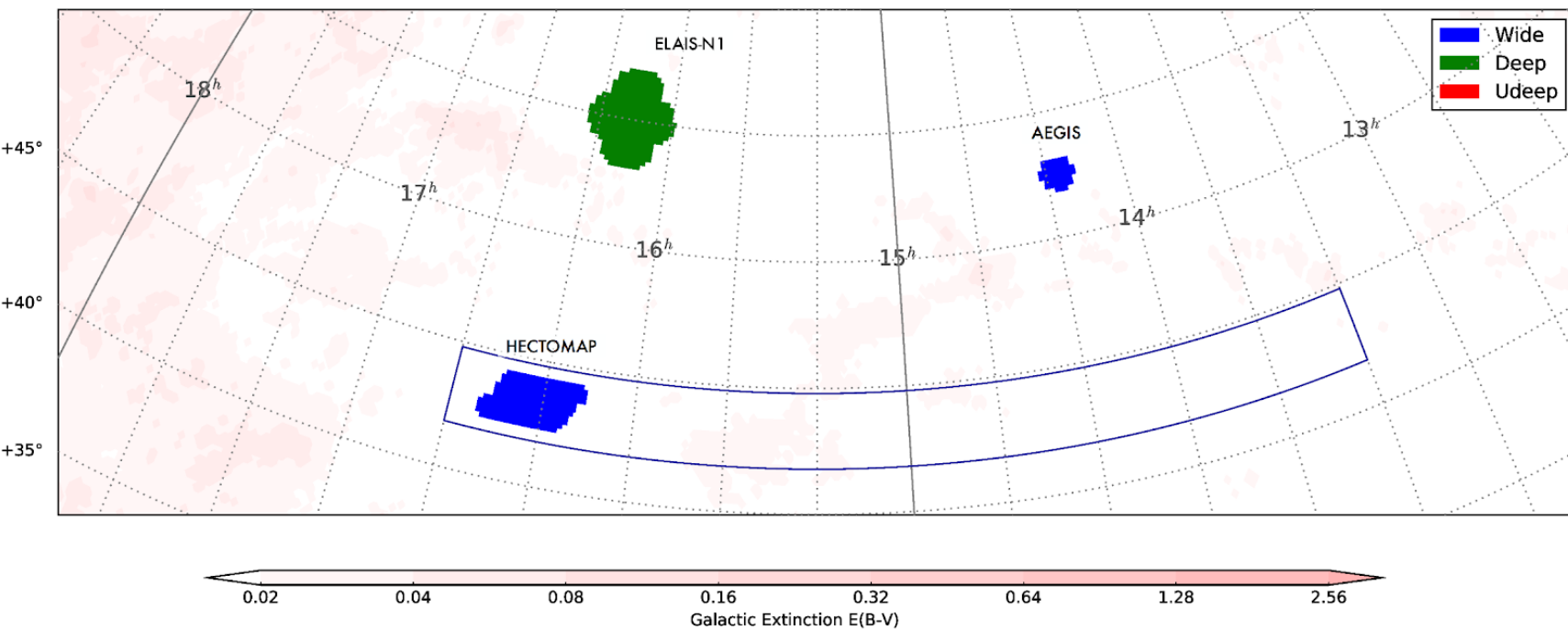
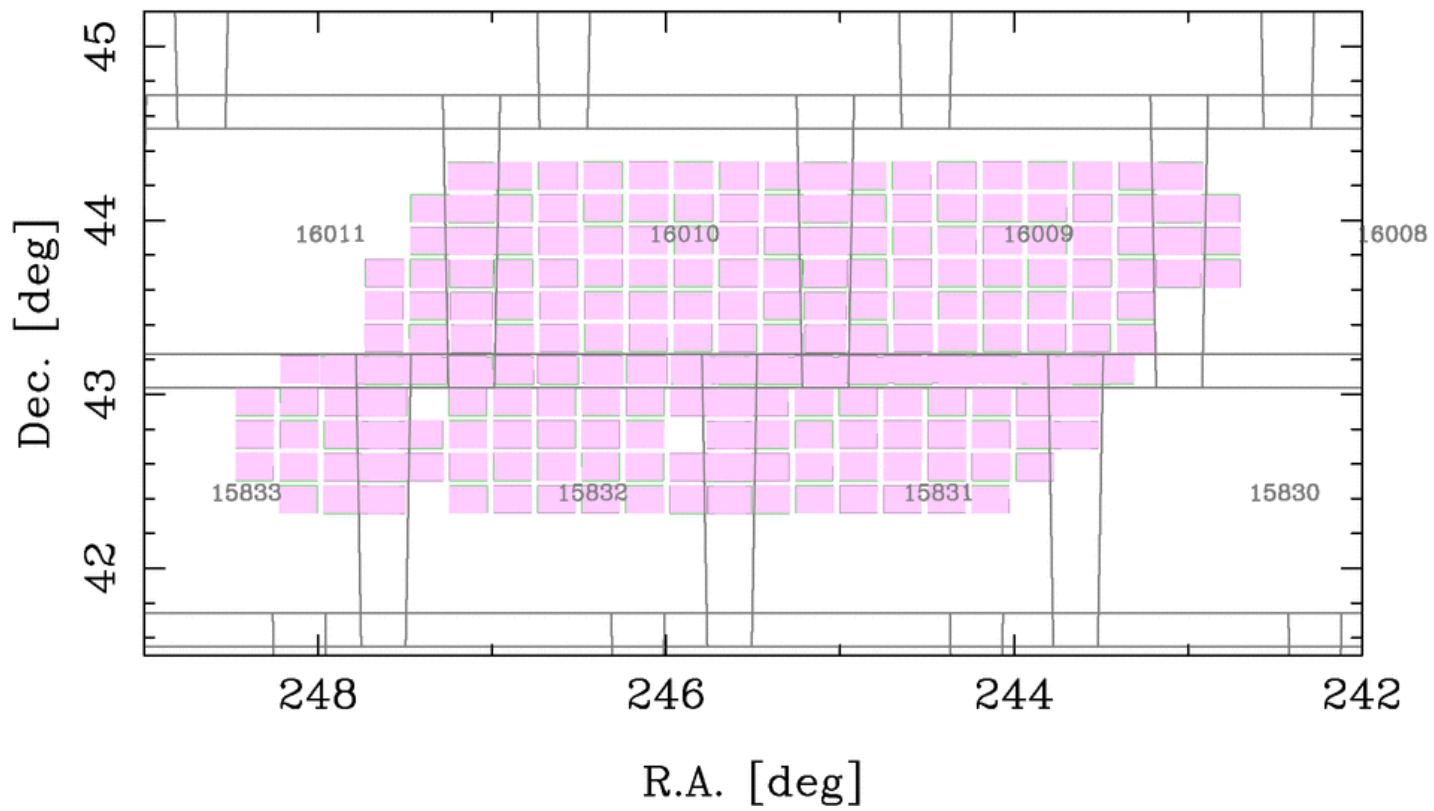


Figure 1: Filters belonging to each filter wheel.



W-HECTOMAP g-band



More details at (arXiv:1403.5237)

J-PAS: The Javalambre-Physics of the Accelerated Universe Astrophysical Survey

N. Benítez^{a,b}, R. Dupke^{b,c,d}, M. Moles^{e,a}, L. Sodré^f, A. J. Cenarro^e, A. Marín-Franch^e, K. Taylor^b,
D. Cristóbal^e, A. Fernández-Soto^l, C. Mendes de Oliveira^f, J. Cepa-Nogué^h, L.R. Abramoⁱ, J.S. Alcaniz^b,
R. Overzier^b, C. Hernández-Monteagudo^e, E. J. Alfaro^a, A. Kanaan^j, J. M. Carvano^b, R. R. R. Reis^k,
E. Martínez González^l, B. Ascaso^a, F. Ballesteros^g, H. S. Xavierⁱ, J. Varela^e, A. Ederoclite^e, H. Vázquez
Ramió^f, T. Broadhurstⁿ, E. Cypriano^f, R. Angulo^e, J. M. Diego^l, A. Zandivarez^o, E. Díaz^o, P. Melchior^p,
K. Umetsu^q, P. F. Spinelli^r, A. Zitrin^s, D. Coe^{an}, G. Yepes^t, P. Vielva^l, V. Sahni^u, A. Marcos-Caballero^l, F. Shu
Kitaura^v, A. L. Maroto^w, M. Masip^{at}, S. Tsujikawa^x, S. Carneiro^y, J. González Nuevo^l, G. C. Carvalho^b,
M. J. Rebouças^{av}, J. C. Carvalho^{b,z}, E. Abdallaⁱ, A. Bernui^b, C. Pigozzo^y, E. G. M. Ferreiraⁱ, N. Chandrachani
Devi^b, C. A. P. Bengaly Jr.^b, M. Campista^b, A. Amorim^g, N. V. Asari^{aa}, A. Bongiovanni^h, S. Bonoli^e,
G. Bruzual^{ab}, N. Cardiel^l, A. Cava^{ac}, R. Cid Fernandes^j, P. Coelho^{ai}, A. Cortesi^f, R. G. Delgado^a, L. Díaz
García^e, J. M. R. Espinosa^h, E. Galliano^b, J. I. González-Serrano^l, J. Falcón-Barroso^h, J. Fritz^{ad},
C. Fernandes^b, J. Gorgas^l, C. Hoyos^f, Y. Jiménez-Teja^{a,b}, J. A. López-Aguerri^h, C. López-San Juan^e,
A. Mateus^l, A. Molino^a, P. Novais^f, A. O'Mill^f, I. Oteo^h, P.G. Pérez-González^l, B. Poggianti^{af}, R. Proctor^b,
E. Ricciardelli^g, P. Sánchez-Blázquez^t, T. Storchi-Bergmann^{ag}, E. Telles^b, W. Schoenell^a, I. Trujillo^h,
A. Vazdekis^h, K. Viironen^e, S. Daflon^b, T. Aparicio Villegas^{b,a}, D. Rocha^{ah}, T. Ribeiro^{ai}, M. Borges^b,
S. L. Martins^{ah}, W. Marcolino^{ah}, D. Martínez-Delgado^{aj}, M.A. Pérez-Torres^f, B.B. Siffert^k, M.O. Calvão^k,
M. Sako^m, R. Kessler^{ak}, A. Álvarez-Candal^b, M. De Prá^b, F. Roig^b, D. Lazzaro^b, J. Gorosábel^a, R. Lopes de
Oliveira^{al}, G. B. Lima-Neto^f, J. Irwin^d, J. F. Liu^{aj}, E. Álvarez^t, I. Balmésⁱ, S. Chueca^e, M.V. Costa-Duarteⁱ,
A. A. da Costaⁱ, M.L.L. Dantas^f, A. Y. Díaz^e, J. Fabregat^g, F. Ferrari^{ao}, B. Gavela^l, S. G. Gracia^f, N. Gruel^{ae},
J. L. L. Gutiérrez^f, R. Guzmán^{ap}, J. D. Hernández-Fernández^e, D. Herranz^h, L. Hurtado-Gil^q, F. Jablonsky^{au},
R. Laporte^{au}, L.L. Le Tiran^f, J. Licandro^h, M. Limaⁱ, E. Martín^{aq}, V. Martínez^g, J. J. C. Montero^f, P. Penteadó^f,
C.B. Pereira^b, V. Peris^g, V. Quilis^g, M. Sánchez-Portal^{ar}, A. C. Soja^f, E. Solano^{ao}, J. Torra^{as}, L. Valdivielso^e

